HOKKAIDO UNIVERSITY

Title	Driving and photo-regulation of myosin–actin motor at molecular and macroscopic level by photo-responsive high energy molecules
Author(s)	Menezes, Halley Mariet
Citation	北海道大学. 博士(生命科学) 甲第12952号
Issue Date	2017-12-25
DOI	10.14943/doctoral.k12952
Doc URL	http://hdl.handle.net/2115/68139
Type	theses (doctoral)
File Information	Halley_Mariet_Menezes.pdf

Instructions for use

Hokkaido University Collection of Scholarly and Academic Papers : HUSCAP

Driving and photo-regulation of myosin-actin motor at molecular and macroscopic level by photo-responsive high energy molecules

（光応答性高エネルギー分子による分子およびマクロレベルでのミオシンーアクチンモーターの駆動と光制御）

A Thesis

Submitted for the Degree of

Doctor of Life Science

By

Halley Mariet Menezes

Laboratory of Smart Molecules

Transdisciplinary Life Science Course

Graduate School of Life Science

Hokkaido University, Japan

December 2017

DECLARATION

I hereby declare that the matter embodied in this thesis entitled **"Driving and photo-regulation of myosin-actin motor at molecular and macroscopic level by photo-responsive high energy molecules"** is the result of investigations carried out by me under the supervision of ***Prof. Nobuyuki Tamaoki*** at the Laboratory of Smart Molecules, Transdisciplinary Life Science Course, Graduate School of Life Science, Hokkaido University, Japan and it has not been submitted elsewhere for the award of any degree or diploma.

In keeping with the general practice of reporting scientific observations, due acknowledgement has been made whenever the work described has been based on the findings of the other investigators. Any omission that might have occurred by oversight or error of judgments is regretted.

Halley Mariet Menezes

CERTIFICATE

I hereby certify that the work described in this thesis entitled **"Driving and photo-regulation of myosin-actin motor at molecular and macroscopic level by photo-responsive high energy molecules"** has been carried out by ***Halley Mariet Menezes***, under my supervision at the Laboratory of Smart Molecules, Transdisciplinary Life Science Course, Graduate School of Life Science, Hokkaido University, Japan.

Prof. Nobuyuki Tamaoki

(Research Supervisor)

TABLE OF CONTENTS

1. INTRODUCTION

Energy of nucleotide hydrolysis fuels the biomolecular motors to lug a myriad of cargos through the cytoplasm and perform a range of cellular tasks.[1,2] A purine nucleotide, adenosine triphosphate (ATP) is hydrolysed by cytoskeleton motors such as myosin, kinesin, dynein and the engendered energy is converted into mechanical work with high efficiency by undergoing conformational changes.[3-5] Harnessing these robust and versatile molecular motors for nanotechnology involves the dynamic control over their motile properties including velocity, direction of motion, processivity and on/off switching.[6-8] Light impelled modulation of ATP function is one of the pronounced approaches towards achieving the motor control.[9-11] Uncaging of inactive caged ATP by photo-irradiation (UV) to switch ON the motility from the OFF state is a remarkable study in this direction.[9] However, the irreversibility of this system made way for the development of high-efficiency reversible ATP analogues to control the motility. In recent past, our group has reported photo-sensitive ATP analogue fuels for reversible control of the motility through illumination with two different wavelengths of light.[12,13]Azobenzene based non-nucleoside triphosphate, AzoTP, in its *trans* state could drive kinesin motor, conversely, the *cis* isomer was unable to drive kinesin; thus facilitating the photo-control of gliding velocity of microtubules on immobilized kinesin between *trans* and *cis* state of AzoTP.

In-vitro motility assays provide an insight into the functioning of motor proteins on a molecular level where the motile interaction of only two isolated proteins under biochemical conditions is studied. Contrary to this, in the physiological macroscopic system motor proteins work collectively in large numbers along with other cellular components or enzymes, thus increasing the number of

interacting molecules.[14-17] In our present study we explore the potential of AzoTP to photo-control such complex macroscopic system of molecular motors, hence extending its applicability over different scales. Myosin II, a muscle protein is a convenient candidate for our study since one of its chief task, muscle contraction, is studied extensively via *in-vitro* motility assay as well as muscle fibre shortening.[18-20] Myosin II ATPase translocates along actin filament and the ATP dependent cyclic sliding interaction between them powers muscle contraction as well as movement.[21,22] To substantiate this concept, glycerol extracted muscle preparation akin to living muscle was developed and evolved over the years to carry out a number of muscle contraction regulation studies.[23] Three-dimensional orderly array of myofilaments and presence of actin-associated proteins like troponin, tropomyosin render the glycerinated muscle fibre system complex than *in-vitro* motility system which involves isolated myosin and actin proteins without an orderly array. Ca^{2+} triggered regulation of glycerinated skeletal muscle fibre contractility is studied extensively.[24,25] However, regulating the contraction by photoisomerizing the substrate locally in the muscle fibre by direct irradiation isn't studied copiously. Recently Christian Hoppmann *et al.* reported the photo-control of living skeletal muscle fibre shortening in which a photo-switchable peptide ligand inhibited the electrically stimulated fibre shortening in *cis* state whilst *trans* state had no effect on shortening.[26]

In this dissertation, we demonstrate the AzoTP triggered driving of myosin and photo-regulation of myosin based macroscopic motile system in glycerinated skeletal muscle fibre by direct photo-irradiation of muscle fibre. *Cis* form of AzoTP fails to initiate significant shortening; following the irradiation with 510nm light, the

muscle fibre shortens remarkably in response to the photo-induced *trans* state. Furthermore we synthesized derivatives of AzoTP and employed them in myosin-actin motile system to investigate the correlation between the structure of substrate and its ability to perform as a photo-responsive energy molecule. We surveyed the efficiency of newly synthesized three derivatives of AzoTP to reversibly photo-control the *in-vitro* actin filament gliding velocity as well as the shortening of glycerinated muscle fibre. The parent AzoTP and its derivatives photo-switched the *in-vitro* motility of actin-myosin between the fast and slow velocity with high efficiency (Fig. 1). Also the shortening of muscle fibre was driven and photo-regulated by these AzoTP molecules, where the photo-irradiation (visible light) induced the shortening in the muscle fibre infused with inactive *cis*-AzoTPs, by locally photo-generated *trans*-AzoTPs ((Fig. 1). Amongst the newly synthesized AzoTP derivatives, the AzoTP with ether group bridging the azobenzene and triphosphate moieties performed as higher efficiency substrate for myosin motor.

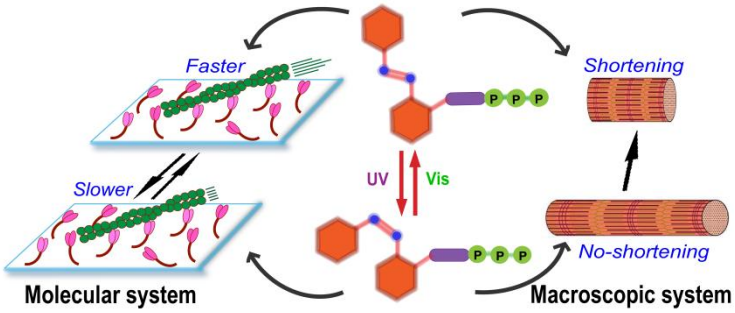

Figure 1. Pictorial representation of the photo-regulation of myosin-actin motile system at molecular (*in-vitro* motility assay) and macroscopic (glycerinated muscle fibre shortening) level.

2. EXPERIMENTAL SECTION

2.1 Materials

Unless otherwise noted, reagents and solvents were used as received from commercial sources (Tokyo Chemical Industry; Watanabe Chemical Industries; Wako Pure Chemical Industries; Dojindo Molecular Technologies) without further purification. Column chromatography was performed on silica gel (60N, spherical, neutral, 40-50 μm), which was purchased from Kanto Chemicals. The ion exchange chromatography was carried out on DEAE Sephadex A-25 packing material, which was purchased from GE Healthcare.

2.2 General methods, instrumentation and measurements

^{1}H, ^{13}C and ^{31}P NMR spectra were recorded using ECX-400 (400 MHz) spectrometer (JEOL). Analysis of the AzoTPs was carried out in a Shimadzu reversed-phase (RP) HPLC system. An EYELA FDU-2200 lyophilisation system was used for freeze-drying. Electrospray ionization time-of-flight Mass Spectrometry (ESI-TOF MS) was performed using a JMS-T100CS instrument (JEOL) operated in the negative-ion mode. High-resolution mass spectrometry was measured on a Thermo Scientific Exactive mass spectrometer with Electrospray Ionization (ESI). Column chromatography was performed using silica gel 60 N (neutral, 60-120 μm, Kanto chemicals). Thin layer chromatography (TLC) was carried out on precoated silica gel 60 F_{254} aluminium sheets (Merck). UV-Vis absorption spectra were recorded using an Agilent 8453 single-beam spectrophotometer and a Shimadzu UV-1800 absorption spectrophotometer. A mercury lamp (Ushio) with band pass filters for 436 and a Hamamatsu LED Controller (model C11924-101) for 365 nm light was used for

photoisomerization and *in-vitro* motility experiments. Hayasaka LED Controller (model CS_LED 3W_510) for 510 nm light was used for photoregulation of *in-situ* motility and muscle fibre shortening experiments. An inverted fluorescence optical microscope (Olympus IX71) equipped with a UPlan F1 100×/1.30 oil C1 objective lens (Olympus) was used for the motility experiments in conjunction with appropriate filters (640 nm excitation filter). An EMCCD digital camera (Andor Solis Technology, model DL-604M-0EM-H1) was used to record videos.

The experiments involving animals (protein extraction) were performed in compliance with the relevant laws and institutional (Hokkaido University, Japan) guidelines.

2.3 Synthesis

The general synthetic route for azobenzene based photochromic non-nucleoside triphosphate molecules involves two major steps; 1) synthesis of hydroxyl attached functional group (R) tethered azobenzenes. 2) Phosphorylation of these functionalized azobenzenes to obtain azobenzene based non-nucleoside triphosphates.

Photochromic non-nucleoside triphosphate, AzoTP was synthesized as described in our previous report. The new derivatives of parent AzoTP, AzoethoxyTP and AzoethylTP were synthesized by functionalizing azobenzene with ethoxy and ethyl groups; likewise DimethylAzoTP was synthesized by functionalizing dimethyl substituted azobenzene with amide group. Synthesis and characterization of these three new derivatives is described in the next sections.

2.3.1 Synthesis of AzoethoxyTP

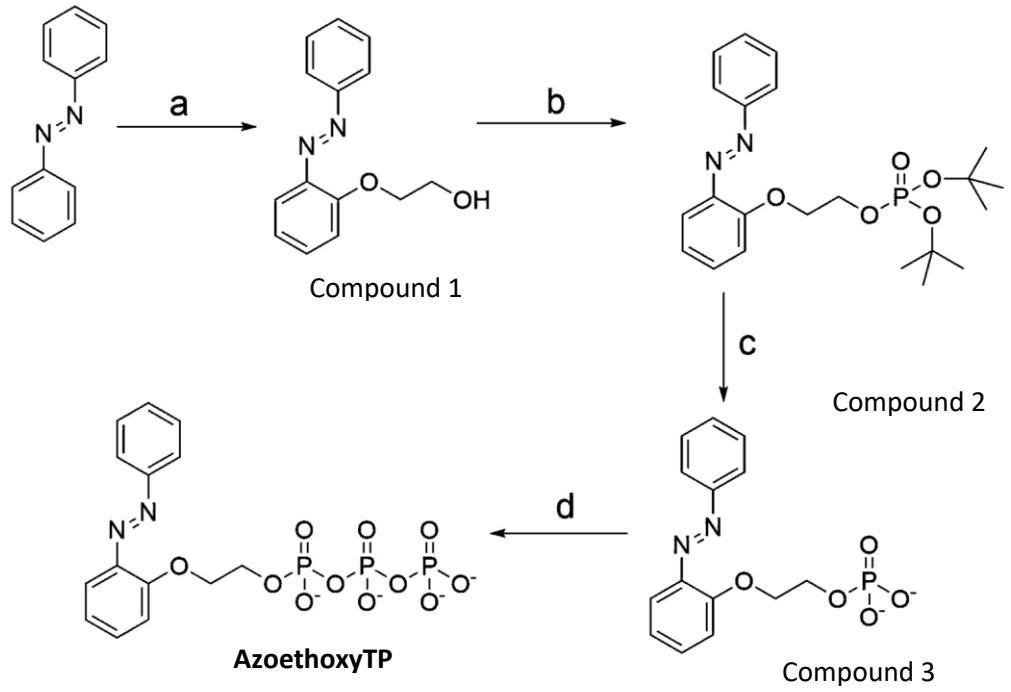

Scheme 1: a) Ethylene glycol, $Pd(OAc)_2$, $PhI(OAc)_2$. **b**) di-*tert*-butyl *N*,*N*-diisopropylphosphoramidite, 1*H*-tetrazole, dry THF, Ar atmosphere, rt, 6h; then, mCPBA,0°C, 1h; then rt, 40 min. **c**) Trifluoroacetic acid, dry CH_2Cl_2, Ar atmosphere, rt, 6 h; then eluting through DEAE Sephadex A-25 anion exchanger, TEAB. **d**) Tributylamine, carbonyldiimidazole, pyrophosphate, dry DMF, Ar atmosphere, rt, overnight.

Compound 1

Azobenezene (1.0 g, 5.49 mmol), $Pd(OAc)_2$ (0.123 g, 0.549 mmol), $PhI(OAc)_2$ (3.536 g, 10.98 mmol), AcOH (6.3 ml, 109.8 mmol) were all added to ethylene glycol (22 ml) in a RB flask and heated at 80^{o}C for 24 h. AcOH was removed by rotary evaporation and the reaction mixture was partitioned between organic (EtOAc) and aqueous layer. The organic phase was dried over $MgSO_4$ and concentrated in a rotary evaporator and the purified compound obtained through column

chromatography (SiO_2, Hexane/EtOAc 7:3). Dark red crystals of compound 1 were obtained (1.03 g, 77%). R_f = 0.33 (Hexane/EtOAc 7:3). Mp: 74.5- 76 °C. ^{1}H NMR [$CDCl_3$, 400MHz]: δ =7.88 (dd, J_1 = 8.3 Hz, J_2 = 2.7 Hz, 2H), 7.69 (dd, J_1 = 8.1 Hz, J_2 = 1.7 Hz, 1H), 7.43-7.52 (m, 4H), 7.18-7.1 (m, 2H), 4.34 (t, J = 4.4 Hz, 2H), 3.96 (q, J = 6.4 Hz, 2H), 3.09 (t, J = 6.5 Hz, 1H). ^{13}C NMR [100.5 MHz, $CDCl_3$] δ = 156.10, 153.00, 143.42, 132.64, 131.18, 129.26, 122.97, 122.24, 118.00, 116.76, 72.55, 61.19. HRMS (ESI, m/z) calculated for $C_{14}H_{16}N_2O_2Na$ $[M + Na]^+$: 265.09475; found: 265.09473 (observed error of -0.07 ppm is within the range of instrumental error of ±5.00 ppm).

Compound 2

1*H*-Tetrazole (0.83 g, 12mmol) was added to a solution of Compound 1 (0.964 g, 4 mmol) and di-*tert*-butyl *N*,*N*-diisopropylphosphoramidite (1.64 mL, 5.2 mmol) in dry THF (20 mL). This reaction mixture was stirred for 6 h at room temperature. A solution of mCPBA (65%) (1.85 g, 6.93 mmol) in dry CH_2Cl_2 (10 mL) was added and stirred for 1h in an ice bath followed by stirring at room temperature for 25 min. Saturated aqueous $NaHCO_3$ was added and the mixture was stirred further for 40 min. The reaction mixture was extracted in an organic (EtOAc) and aqueous solution (NaCl). The organic phase separated, dried over $MgSO_4$ and concentrated in a rotary evaporator, passed through column chromatography to obtain the purified reddish viscous liquid of Compound 2. Yield = 0.15 g (14%). R_f = 0.10 (Hexane/EtOAc 7:3). ^{1}H NMR ($CDCl_3$, 400 MHz): δ = 8.6 (br, 1H), 7.91 (d, J = 8.0 Hz, 2H), 7.65 (d, J = 8.0 Hz, 1H), 7.52−7.40 (m, 4H), 7.12 (d, J = 8.2 Hz 1H), 7.05 (t, J = 7.6 Hz, 1H), 4.43 – 4.37 (m, 4H), 1.46 (s, 18 H). ^{13}C NMR [100.5 MHz, $CDCl_3$] δ 156.22, 153.07, 142.88, 132.38, 130.89, 129.05, 123.12, 121.64, 117.13, 115.34, 82.66 (d, J = 7.4

Hz), 68.99(d, *J* = 8.5 Hz), 64.95 (d, *J* = 6.0 Hz), 29.88 (d, *J* = 4.3 Hz). HRMS (ESI, m/z) calculated for $C_{22}H_{31}N_2O_5PNa$ $[M + Na]^+$: 457.18628; found: 457.18634 (observed error of 0.13 ppm is within the range of instrumental error of ±5.00 ppm).

Compound 3

Trifluoroacetic acid (0.4 mL, 5.5 mmol) was added to the solution of compound 2 (0.15 g, 0.34 mmol) in dry CH_2Cl_2 (3 mL) and stirred for 6 h at room temperature followed by solvent evaporation. For the complete removal of CF_3COOH, the procedure of addition of MeOH and evaporation was repeated thrice followed by CH_2Cl_2 wash. Vacuum dried the obtained residue of monophosphate and dissolved in water by adjusting the pH to 7.5 using 1M NaOH. This solution was eluted through a DEAE Sephadex A-25 column with 0.5M triethylammonium hydrogencarbonate solution at 4 °C to convert the monophosphate into its triethylammonium salt. Triethyl ammonium hydrogencarbonate was removed by evaporation with EtOH several times to afford 0.11 g (96% yield) of Compound 3 as triethyl ammonium salt. ^{1}H NMR (CD_3OD, 400 MHz): δ = 9.27 (br, 1H), 7.91 (d, *J* = 6.9 Hz, 2H), 7.64 (d, *J* = 8.0 Hz, 1H), 7.55 – 7.45 (m, 4H), 7.26 (d, *J* = 8.3 Hz, 1H), 7.06 (t, *J* = 8.2 Hz, 1H), 4.43 (t, *J* = 5.1 Hz, 2H), 4.39 – 4.37 (m, 2H). ^{13}C NMR [100.5 MHz, CD_3OD] δ 157.72, 154.39, 143.83, 133.81, 132.08, 130.21, 123.98, 122.57, 117.84, 116.57, 70.48 (d, *J* = 7.7 Hz), 66.06 (d, *J* = 5.4 Hz). HRMS (ESI, m/z) calculated for $C_{14}H_{14}N_2O_5P$ $[M - H]^-$: 321.06458; found: 321.06483 (observed error of 0.77 ppm is within the range of instrumental error of ±5.00 ppm).

AzoethoxyTP

The triethylammonium salt of Compound 3 (0.1 g, 0.236 mmol) was converted into its tributylammonium salt through the addition of tributylamine (0.2 mL, 0.787 mmol) in dry MeOH (1.4 mL). Triethylamine and MeOH were removed through

rotary evaporation. The tributylammonium salt was dissolved in dry DMF (2.4 mL), a solution of 1,1´-carbonyldiimidazole (0.24 g, 1.48 mmol) in dry DMF (2.0 mL) was added under Ar atmosphere with stirring and then kept at room temperature for 16 h to proceed the reaction. Excess of 1,1´-carbonyldiimidazole was destroyed by the addition of dry MeOH (0.06 mL, 0.06 mmol) and stirring for 1hr. This solution was then added dropwise with stirring to a solution of the tributylammonium salt of pyrophosphate (0.69 g, 1.48 mmol) in dry DMF (2.0 mL). After reacting overnight at room temperature, the mixture was cooled to 0°C in an ice bath. Cold water (4°C) was added with stirring and the pH was brought to 7.5 using 1M NaOH. The reaction mixture was extracted with ether and H_2O; the aqueous phase was evaporated with EtOH at 30°C and dried. The residue was dissolved in 0.2 M triethylammonium hydrogencarbonate , applied to a DEAE-Sephadex A-25 column (2.5 × 30 cm, 20 g) and eluted with a linear gradient (0.2–1.0 M; total volume: 1 L) of triethylammonium hydrogencarbonate at 4°C. The product eluted in the 0.67–0.86 M range was collected and evaporated with EtOH several times to remove triethylammonium hydrogencarbonate. The obtained residue of product was converted into its sodium salt using 1M NaI in acetone and freeze dried. Yield = 0.05 g (44%). Mp 161-163 °C. ^{1}H NMR (D_2O, 400 MHz): δ = 7.27 (d, *J* = 6.6 Hz, 2H), 7.06 – 7.02 (m, 5H), 6.86 (d, *J* = 7.0 Hz, 1H), 6.69 (t, *J* = 6.6 Hz, 1H), 4.56 (m, 2H), 4.48 (m, 2H). ^{13}C NMR [100 MHz, D_2O (CD_3OD)] δ 156.22, 153.33, 142.86, 134.54, 132.67, 130.48, 123.58, 122.92, 118.18, 116.19, 70.16 (d, *J* = 7.9 Hz), 65.71 (d, *J* = 5.2 Hz). ^{31}P NMR [160 MHz, D_2O (H_3PO_4)] δ -10.89 – -11.20 (m, 2P), -23.03 – -23.19 (m, 1P). HRMS (ESI, m/z) calculated for $C_{14}H_{14}N_2O_{11}Na_4P_3$ $[M + H]^+$: 570.93957; found: 570.93993 (observed error of 0.62 ppm is within the range of instrumental error of ±5.00 ppm).

2.3.2 Synthesis of DimethylazoTP

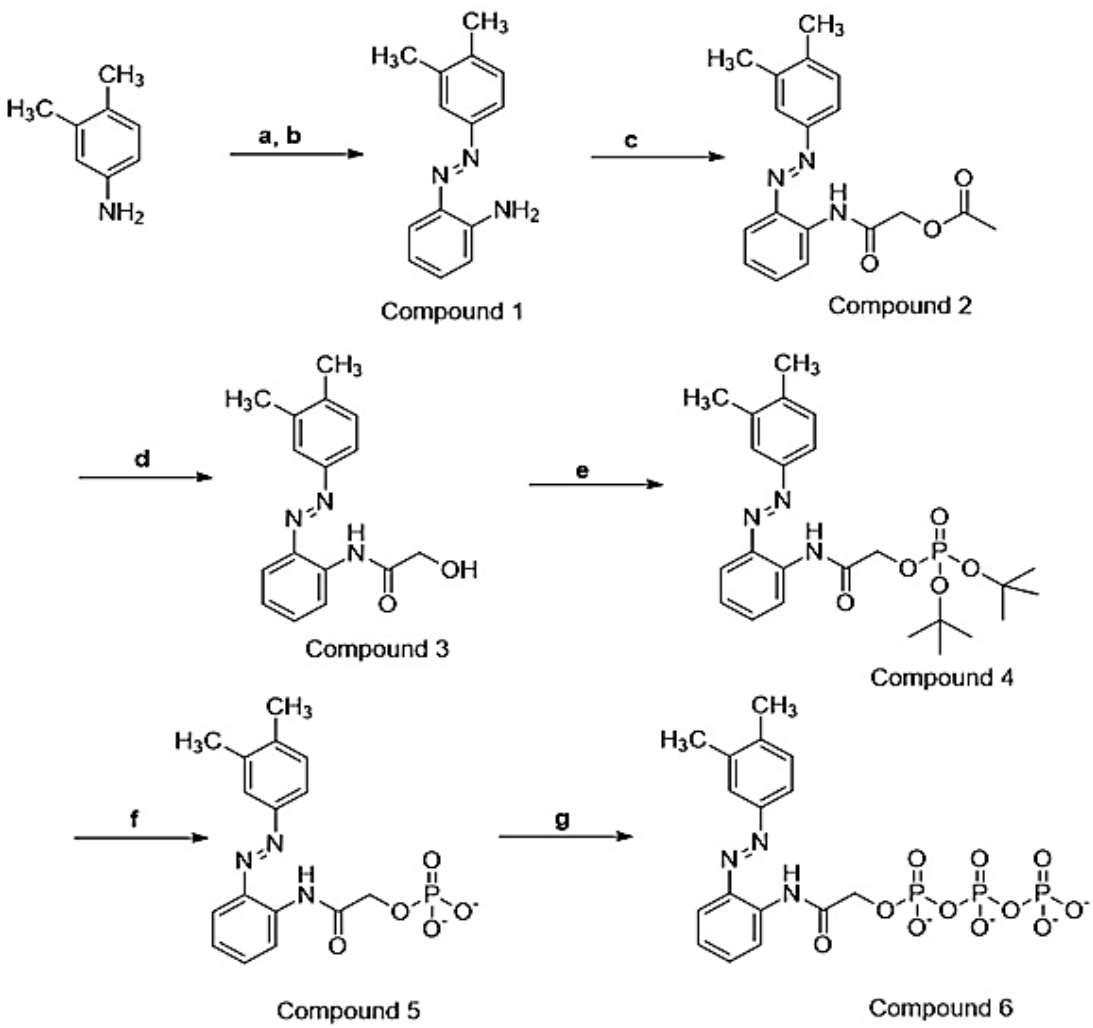

Scheme 2: a) mCPBA, EtOAc, 0°C, 3h. **b**) 1,2-phenylenediamine, AcOH, EtOAc, N_2- atmosphere, 50 °C, 72h. **c**) Acetoxyactyl chloride, Triethylamine, DCM, RT, 3h. **d**) K_2CO_3, MeOH, RT, Overnight. **e**) Di-*tert*-butyl *N*,*N*-Diisopropylphosphoramidite, 1H-tetrazol, dry THF, Ar-atmosphere, RT, 6h, then mCPBA, 0°C,1h. **f**) TFA, dry DCM, Ar-atmosphere, RT, 6h. **g**) Tributylamine, carbonyldiimidazole, tributylammonium pyrophosphate, dry DMF, Ar-atmosphere, RT, overnight.

Compound 1

m-CPBA (9.40g, 60.02 mmol) was added to a solution of 3,4-dimethylaniline (3.64g, 30 mmol) in EtOAc (300 mL) at 0 °c in ice bath. The reaction mixture was stirred for 3 hours then extracted with EtOAc and sat. NaHCO3 then washed with water. Organic part was dried with $MgSO_4$. Then reduced the volume using a *rotovap*. When the volume was reached to approx. 150 mL the evaporation was stopped and the solution was degassed with dry N_2 for 15 min. Then 1,2-phenylenediamine (3.2g, 30 mmol) and acetic acid (1mL) were added to the solution under N_2-atmosphere. The reaction mixture was stirred at 50 °c for 89 h. After 89 h the reaction mixture was extracted with water and EtOAc. The organic part was dried with $MgSO_4$ and concentrated in a *rotovap*. The residue was purified by silica gel column chromatography. The compound was eluted with hexane/EtOAc, 9:1 to afford dark red crystals of Compound 1. Yield = 2.70 g (40%). R_f = 0.30 (Hexane/EtOAc 9:1).Mp: 128-130 °C. ^{1}H NMR [400MHz, $CDCl_3$] δ 7.80 (dd, *J* = 8.1, 1.5 Hz, 1H), 7.63 – 7.58 (m, 2H), 7.25 – 7.17 (m, 2H), 6.81 (ddd, *J* = 8.2, 7.1, 1.3 Hz, 1H), 6.76 (dd, *J* = 8.2, 1.1 Hz, 1H), 5.83 (br, 2H), 2.35 (s,3H), 2.33 (s, 3H). ^{13}C NMR [100.5 MHz, $CDCl_3$] δ 151.42, 142.99, 139.27, 137.46, 137.26, 131.94, 130.34, 127.27, 123.14, 120.10, 117.49, 117.06, 20.03, 19.92. HRMS (ESI, m/z) calculated for $C_{14}H_{16}N_3$ $[M + H]^+$: 226.13387; found: 226.13383 (observed error of -0.19 ppm is within the range of instrumental error of ±5.00 ppm).

Compound 2

Triethyl amine (2.54 mL, 18.15 mmol) was added to a solution of Compound 1 (2.70 g, 12.10 mmol) in DCM (90 mL) at 0 °c in ice bath. While stirring, acetoxyactyl chloride (1.95 mL, 18.15 mmol) was added dropwise to the reaction mixture at 0 °c in ice bath. Then the reaction mixture was kept 15 min in ice bath than in room

temperature for 3 h. The reaction mixture was extracted with DCM and water. The organic part was dried with $MgSO_4$ and all the solvents were removed using a *rotovap*. The residue was purified by washing with hexane several times and DCM twice and finally dried in vacuum to afford 3.51 g (89%) of orange solid compound 2. $R_{f\,=}$ 0.1 (Hexane/EtOAc 9:1). Mp 148-149 °C. ^{1}H NMR (400 MHz, DMSO-D6) δ 10.23 (s, 1H), 8.32 (dd, *J* = 8.3, 1.1 Hz, 1H), 7.82 – 7.71 (m, 3H), 7.56 – 7.52 (m, 1H), 7.38 (d, *J* = 8.1 Hz, 1H), 7.28 – 7.24 (m, 1H), 4.81 (s, 2H), 2.35 (s, 3H), 2.33 (s, 3H), 2.15 (s, 3H). ^{13}C NMR [100.5 MHz, DMSO-D6] δ 169.74, 165.85, 150.57, 141.03, 140.70, 137.55, 136.00, 132.25, 130.35, 124.41, 124.20, 121.79, 120.47, 116.42, 63.00, 20.53, 19.54, 19.45. HRMS (ESI, m/z) calculated for $C_{18}H_{19}N_3O_3Na$ $[M + Na]^+$: 348.13186; found: 348.13154 (observed error of -0.93 ppm is within the range of instrumental error of ±5.00 ppm).

Compound 3

K_2CO_3 (2.79g, 20.0 mmol) was added to a solution of compound 2 (3.48g, 10.69 mmol) in MeOH/DMSO (40mL+10mL) at room temperature. The reaction mixture was stirred for overnight. Then the reaction mixture was partitioned with EtOAc and water. The EtOAc part was dried with $MgSO_4$ and all the solvents were removed using a *rotovap*. The residue was washed with hexane several times and DCM twice finally dried under vacuum to afford 2.91 g (96%) of compound 3. $R_{f\,=}$ 0.13 (Hexane/EtOAc 7:3). Mp 170-172 °C. ^{1}H NMR (400 MHz, DMSO-D6) δ 11.10 (s, 1H), 8.64 (dd, *J* = 8.4, 1.1 Hz, 1H), 7.82 – 7.77 (m, 2H), 7.71 (dd, *J* = 8.0, 2.0 Hz, 1H), 7.58 – 7.53 (m, 1H), 7.39 (d, *J* = 8.0 Hz, 1H), 7.27 – 7.23 (m, 1H), 6.40 (s, 1H), 4.09 (s, 2H), 2.34 (s, 3H), 2.33 (s, 3H). ^{13}C NMR [100.5 MHz, DMSO-D6] δ 170.99, 150.42, 141.22, 138.78, 137.73, 135.46, 132.77, 130.53, 123.65, 123.26, 120.67,

119.42, 118.95, 61.98, 19.59, 19.56. HRMS (ESI, m/z) calculated for $C_{16}H_{17}N_3O_2Na$ $[M + Na]^+$: 306.12130; found: 306.12127 (observed error of -0.09 ppm is within the range of instrumental error of ±5.00 ppm).

Compound 4

1*H*-Tetrazole (1.59 g, 23.07 mmol) was added to a solution of compound 3 (2.18 g, 7.69 mmol) and di-*tert*-butyl *N*,*N*-diisopropylphosphoramidite (3.15 mL, 9.99 mmol) in dry THF (40 mL) in Ar-atmosphere and then the mixture was stirred for 7 h at room temperature. A solution of *m*-CPBA (65%, 3.56 g, 13.32 mmol) in dry CH_2Cl_2 (20 mL) was added; the mixture was stirred for 1 h in an ice bath and then for 30 min at room temperature. Saturated aqueous $NaHCO_3$ (90 mL) was added and the mixture was stirred for a further 30 min. The reaction mixture was partitioned between EtOAc and water. The organic phase was washed with aqueous solutions of NaCl (once), dried (with $MgSO_4$) and concentrated in *rotovap*. The residue was purified through silica gel column chromatography. The compound was eluted with hexane/EtOAc, 3:2 to afford 1.54 g (42%) of Compound **4**. R_f = 0.25 (Hexane/EtOAc 7:3). Mp: 132-133 °C. ^{1}H NMR (400 MHz, $CDCl_3$): δ = 10.71 (s, 1H), 8.69 (dd, J_1 = 8.4 Hz, J_2= 1.2 Hz, 1H), 7.87 – 7.80 (m, 3H), 7.49 – 7.45 (m, 1H), 7.31 (d, J = 7.8 Hz, 1H), 7.23 – 7.18 (m, 1H), 4.60 (d, J = 7.0 Hz, 2H), 2.41 (s, 3H), 2.35 (s, 3H), 1.46 (s, 18H). ^{13}C NMR [100.5 MHz, $CDCl_3$] δ 166.16 (d, J = 8.9 Hz), 150.95, 141.13, 139.82, 137.72, 135.50, 132.30, 130.64, 125.38, 124.21, 120.27, 120.30, 118.56, 83.64 (d, J = 7.1 Hz), 65.72 (d, J = 6.7 Hz), 29.92 (d, J = 4.2 Hz), 20.04, 19.90. HRMS (ESI, m/z) calculated for $C_{24}H_{34}N_3O_5PNa$ $[M + Na]^+$: 498.21283; found: 498.21237 (observed error of -0.92 ppm is within the range of instrumental error of ±5.00 ppm).

Compound 5

Trifluoroacetic acid (2.16 mL) was added to a solution of compound 4 (0.84 g, 1.77 mmol) in dry DCM (20 mL) and then the mixture was stirred for 6 h at room temperature. MeOH (30 mL) was added and then the mixture was evaporated; this procedure was repeated three more times to remove CF_3COOH completely, followed by washing with CH_2Cl_2. All solvents were removed using a *rotovap* and the residue was dried under vacuum. Water was added to the residue and neutralized with 1 M NaOH. Crude product was purified by DEAE Sephadex A-25 column. The compound was eluted using 0.5 M triethylammonium hydrogencarbonate (TEAB) solution at 4 °C. The fractions containing the product were coevaporated with EtOH using a *rotovap* and the residue was dried under vacuum to afford 0.77 g (94%) of Compound 5 as triethyl ammonium salt. Mp: 139-141°C. ^{1}H NMR (CD_3OD, 400 MHz): δ = 8.58 (dd, *J* = 8.3, 1.1 Hz, 1H), 7.90 – 7.82 (m, 3H), 7.49 – 7.46 (m, 1H), 7.36 (d, *J* = 8.0 Hz, 1H), 7.24 – 7.19 (m, 1H), 4.54 (d, *J* = 6.1 Hz, 2H), 3.17 (q, *J* = 7.3 Hz, 6H), 2.41 (s, 3H), 2.35 (s, 3H), 1.28 (t, *J* = 7.3 Hz, 9H). ^{13}C NMR [100.5 MHz, CD_3OD] δ 169.94 (d, *J* = 9.1 Hz), 152.27, 142.33, 141.41, 138.92, 137.07, 133.06, 131.83, 127.02, 125.30, 121.50, 120.88, 118.24, 65.71 (d, *J* = 4.7 Hz), 47.71, 19.94, 19.86, 9.16. HRMS (ESI, m/z) calculated for $C_{16}H_{17}N_3O_5P$ [M – $C_6H_{17}N$(TEA)]$^-$: 362.09113; found: 362.09140 (observed error of 0.74 ppm is within the range of instrumental error of ±5.00 ppm).

DimethylAzoTP

The triethylammonium salt of compound 5 (0.37g, 0.79 mmol) was converted to its tributylammonium salt through the addition of tributylamine (0.75 mL, 3 mmol) in dry MeOH (5 mL). Triethylamine and MeOH were removed through *rotovap*. The

tributylammonium salt was dissolved in dry DMF (8 mL). While stirring, a solution of 1,1´-carbonyldiimidazole (0.61 g, 3.76 mmol) in dry DMF (5 mL) was added under Ar-atmosphere and then the reaction was left for 16 h at room temperature. Excess 1,1´-carbonyldiimidazole was destroyed through the addition of dry MeOH (0.12 mL, 2.96 mmol) and stirring for 1 h. This solution was added dropwise with mixing to a solution of the tributylammonium salt of pyrophosphate, (prepared from tetrasodium pyrophosphate) (1.31g, 4.93 mmol) in dry DMF (5 mL). After reacting overnight at room temperature, the mixture was cooled to 0 °C in an ice bath. Cold water (15 mL, 4 °C) was added with mixing and then the pH was brought to 7.5 using 1 M NaOH. The reaction mixture was partitioned between ether and H_2O; the aqueous phase was coevaporated with EtOH at 30 °C and dried in a *rotovap*. Crude product was purified by DEAE Sephadex A-25 column. The compound was eluted using a linear gradient of 0.2-1.0 M TEAB solution at 4 °C. The fractions containing the product as confirmed using ESI MS were coevaporated with EtOH by using a *rotovap* and the residue was dried under vacuum. The obtained product was dissolved in dry MeOH (1mL) upon addition of NaI in acetone (1M, 10mL) sodium salt of the product was precipitated. The precipitated was washed several times with acetone and dried by lyophilizer to afford 0.46 g (95%) of DimethylazoTP as sodium salt. Mp 168-170 °C. ^{1}H NMR (D_2O, 400 MHz): δ = 7.95 (d, *J* = 7.1 Hz, 1H), 7.76 – 7.68 (m, 3H), 7.63 – 7.59 (m, 1H), 7.45 – 7.40 (m, 2H), 4.69 (d, *J* = 7.4 Hz, 2H), 2.39 (s, 3H), 2.36 (s, 3H). ^{13}C NMR [100 MHz, D_2O (CD_3OD)] δ = 170.93 (d, *J* = 9.6 Hz), 151.35, 143.78, 143.16, 139.35, 134.64, 133.11, 131.58, 127.47, 125.56, 124.48, 120.54, 118.18, 65.73 (d, *J* = 5.6 Hz), 20.03, 19.92. ^{31}P NMR [160 MHz, D_2O (H_3PO_4)] δ -10.90 (d, 1P, *J* = 18.6 Hz), -12.48 (d, 1P, *J* = 19.3 Hz), -23.06 (t, 1P, *J* = 17.8 Hz).

HRMS (ESI, m/z) calculated for $C_{16}H_{17}N_3O_{11}Na_4P_3$ $[M + H]^+$: 611.96612; found: 611.96757 (observed error of 2.36 ppm is within the range of instrumental error of ±5.00 ppm).

2.3.3 Synthesis of AzoethylTP

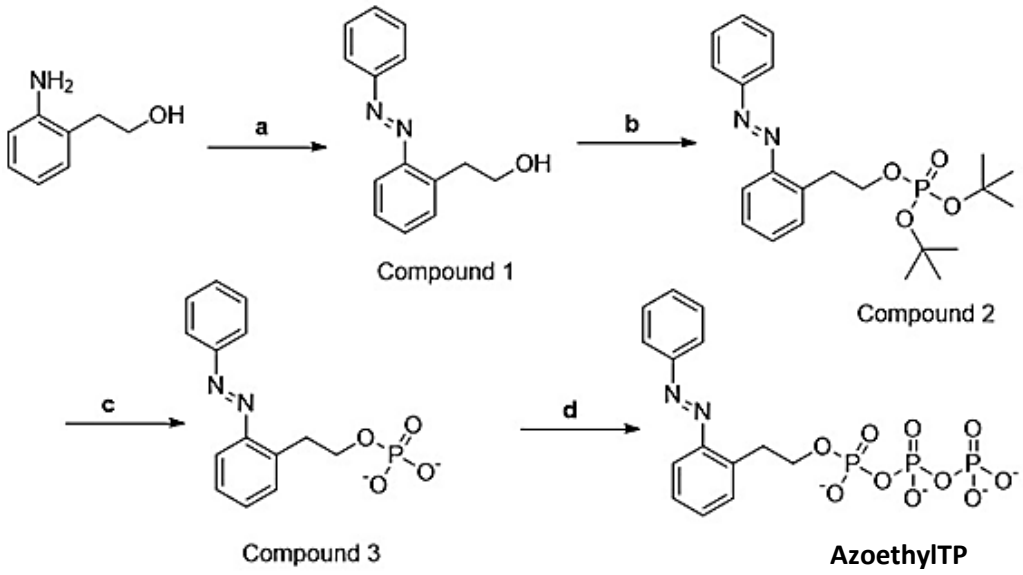

Scheme 3: a) ArNO, AcOH, Toluene, Ar-atmosphere, 60 °C, 72h. **b)** Di-*tert*-butyl *N*,*N*-Diisopropylphosphoramidite, 1H-tetrazol, dry THF, Ar-atmosphere, RT, 6h, then mCPBA, 0°C, 1h. **c)** TFA, dry DCM, Ar-atmosphere, RT, 6h. **d)** Tributylamine, carbonyldiimidazole, tributylammonium pyrophosphate, dry DMF, Ar atmosphere, RT, overnight.

Compound 1

A solution of 2-(2-Aminophenyl) ethanol (4.65 g, 33.90 mmol) in toluene (200 mL) was degassed under a stream of N_2 for 15 min then nirtosobenzene (3.63 g, 33.89 mmol) and acetic acid (0.8 mL) were added under Ar-atmosphere. The reaction mixture was stirred at 60 °C for 72h. The solvent of the reaction mixture was evaporated in *rotovap* and partitioned between water and DCM. The DCM part was

dried (with $MgSO_4$) and concentrated in a *rotovap*. The residue was purified by silica gel column chromatography. The compound was eluted with hexane/EtOAc, 3:2 to afford 5.75 g (75%) of Compound 1. R_f = 0.30 (Hexane/EtOAc 7:3).^{1}H NMR [400MHz, $CDCl_3$]: δ 7.91 – 7.88 (m, 2H), 7.71 (dd, , J_1 = 8.0 Hz, J_2 = 1.0 Hz, 1H), 7.55 – 7.45 (m, 3H), 7.44 – 7.39 (m, 2H), 7.37 – 7.33 (m, 1H), 3.96 (dd, J_1 = 12.2 Hz, J_2 = 6.4 Hz, 2H), 3.40 (t, J = 6.4 Hz, 2H), 2.02 (t, J = 5.6 Hz, 1H). ^{13}C NMR [100.5 MHz, $CDCl_3$] δ 152.72, 150.55, 138.70, 131.34, 131.23, 131.08, 129.14, 127.29, 122.94, 115.72, 63.87, 35.09. HRMS (ESI, m/z) calculated for $C_{14}H_{14}N_2ONa$ $[M + Na]^+$: 249.09983; found: 249.09957 (observed error of -1.06 ppm is within the range of instrumental error of ±5.00 ppm).

Compound 2

1*H*-Tetrazole (1.66 g, 24.0 mmol) was added to a solution of compound 1 (1.82 g, 8.04 mmol) and di-*tert*-butyl *N*,*N*-diisopropylphosphoramidite (3.3 mL, 10.4 mmol) in dry THF (40 mL) and then the mixture was stirred for 7 h at room temperature. A solution of *m*-chloroperoxybenzoic acid (65%, 3.70 g, 13.86 mmol) in dry CH_2Cl_2 (20 mL) was added; the mixture was stirred for 1 h in an ice bath and then for 30 min at room temperature. Saturated aqueous $NaHCO_3$ (90 mL) was added and the mixture was stirred for a further 30 min. The reaction mixture was partitioned between EtOAc and water. The organic phase was washed with aqueous solutions of NaCl (once), dried (with $MgSO_4$) and concentrated in *rotovap*. The residue was purified through silica gel column chromatography. The compound was eluted with hexane/EtOAc, 3:2 to afford 1.30 g (38%) of Compound 2. R_f = 0.19 (Hexane/EtOAc 7:3). ^{1}H NMR (400 MHz, $CDCl_3$): δ = 7.93 – 7.90 (m, 2H), 7.70 (d, J = 7.6 Hz 1H), 7.54 – 7.39 (m, 3H), 7.43 – 7.39 (m, 2H), 7.36 – 7.31 (m, 1H), 4.23 (q, J = 7.1 Hz,

2H), 3.53 (t, *J* = 7.2 Hz, 2H), 1.40 (s, 18H). ^{13}C NMR [100.5 MHz, $CDCl_3$] δ 152.82, 150.45, 137.49, 131.52, 131.16, 131.02, 129.08, 127.52, 123.03, 115.46, 82.09 (d, *J* = 7.3 Hz), 67.55 (d, *J* = 6.7 Hz), 32.73 (d, *J* = 8.0 Hz), 29.77 (d, *J* = 4.2 Hz). HRMS (ESI, m/z) calculated for $C_{22}H_{31}N_2O_4PNa$ $[M + Na]^+$: 441.19137; found: 441.19107 (observed error of -0.67 ppm is within the range of instrumental error of ±5.00 ppm).

Compound 3

Trifluoroacetic acid (3.50 mL) was added to a solution of compound 2 (1.20 g, 2.86 mmol) in dry CH_2Cl_2 (32 mL) and then the mixture was stirred for 6 h at room temperature. MeOH (30 mL) was added and then the mixture was evaporated; this procedure was repeated three more times to remove CF_3COOH completely, followed by washing with CH_2Cl_2. All solvents were removed using a *rotovap* and the residue was dried under vacuum. Water was added to the residue and neutralized with 1 M NaOH. Crude product was purified by DEAE Sephadex A-25 column. The compound was eluted using 0.5 M triethylammonium hydrogencarbonate (TEAB) solution at 4 °C. The fractions containing the product were coevaporated with EtOH using a *rotovap* and the residue was dried under vacuum to afford 0.59 g (51%) of Compound 3 as triethyl ammonium salt. Mp: 130-132 °C. ^{1}H NMR (CD_3OD, 400 MHz): δ = 7.94 – 7.92 (m, 2H), 7.67 (dd, *J* = 8.1, 1.2 Hz, 1H), 7.56 – 7.49 (m, 4H), 7.43 (td, *J* = 7.4, 1.3 Hz, 1H), 7.32 – 7.29 (m, 1H), 4.14 (dd, *J* = 14.0, 7.3 Hz, 2H), 3.51 (t, *J* = 7.4 Hz, 2H), 3.16 (q, *J* = 7.3 Hz, 6H), 1.28 (t, *J* = 7.3 Hz, 9H). ^{13}C NMR [100.5 MHz, CD_3OD] δ 154.31, 151.69, 139.79, 132.72, 132.41, 132.24, 130.31, 128.36, 124.00, 116.18, 67.24, 59.54, 34.02, 8.12. HRMS (ESI, m/z) calculated for $C_{14}H_{14}N_2O_4P$ $[M - C_6H_{16}N(TEA)]^-$: 305.06967; found: 305.06991 (observed error of 0.13 ppm is within the range of instrumental error of ±5.00 ppm).

AzoethylTP

The triethylammonium salt of compound 3 (0.20g, 0.50 mmol) was converted to its tributylammonium salt through the addition of tributylamine (0.5 mL, 2 mmol) in dry MeOH (2.5 mL). Triethylamine and MeOH were removed through *rotovap*. The tributylammonium salt was dissolved in dry DMF (5 mL). While stirring, a solution of 1,1´-carbonyldiimidazole (0.36 g, 2.22 mmol) in dry DMF (3 mL) was added under Ar-atmosphere and then the reaction was left for 16 h at room temperature. Excess 1,1´-carbonyldiimidazole was destroyed through the addition of dry MeOH (0.070 mL, 1.7 mmol) and stirring for 1 h. This solution was added dropwise with mixing to a solution of the tributylammonium salt of pyrophosphate, (prepared from tetrasodium pyrophosphate) (0.83 g, 3.12 mmol) in dry DMF (5 mL). After reacting overnight at room temperature, the mixture was cooled to 0 °C in an ice bath. Cold water (15 mL, 4 °C) was added with mixing and then the pH was brought to 7.5 using 1 M NaOH. The reaction mixture was partitioned between ether and H_2O; the aqueous phase was evaporated with EtOH at 30 °C and dried. Crude product was purified by DEAE Sephadex A-25 column. The compound was eluted using a linear gradient of 0.2-1.0 M TEAB solution at 4 °C. The fractions containing the product as confirmed using ESI MS were mix with EtOH and evaporated using a *rotovap* and the residue dried under vacuum. The obtained product was dissolved in dry MeOH (1mL) upon addition of NaI in acetone (1M, 10mL) sodium salt of the product was precipitated. The precipitated was washed several times with acetone and dried by lyophilizer to afford 0.181 g (64%) of AzoethylTP as sodium salt. Mp 153-155 °C. ^{1}H NMR (400 MHz, D_2O) δ 7.96 – 7.93 (m, 2H), 7.64 – 7.59 (m, 3H), 7.56 – 7.52 (m, 2H), 7.44 – 7.41 (m, 1H), 4.24 (q, *J* = 8.0 Hz, 2H), 3.48 (t, *J* = 6.9 Hz, 2H). ^{13}C

NMR [100 MHz, D_2O (CD_3OD)] δ = 153.31, 151.51, 138.15, 132.69, 132.60, 130.51, 128.75, 123.67, 116.61, 68.12 (d, *J* = 6.1 Hz), 32.82 (d, *J* = 6.8 Hz). ^{31}P NMR [160 MHz, D_2O (H_3PO_4)] δ -10.71 – -11.19 (m, 2P), -23.28 (t, 1P, *J* = 19.6 Hz). HRMS (ESI, m/z) calculated for $C_{14}H_{14}N_2O_{10}Na_4P_3$ $[M + H]^+$: 554.94466; found: 554.94501 (observed error of 0.63 ppm is within the range of instrumental error of ±5.00 ppm).

2.4 Characterization of AzoTP derivatives

2.4.1 HPLC profile of AzoTP molecules

The purity of parent AzoTP (**1**) and its newly synthesized derivatives (**2** – **4**) was confirmed by RP-HPLC analysis. The conditions maintained - column: CN-80Ts, 4.6 × 250 mm (TOSOH); eluent: CH_3CN / NaPi buffer (pH 6.5); solvent gradient: 15 – 45% of CH_3CN in NaPi buffer; monitoring wavelength: λ= 327 nm; flow rate: 0.5 mL / min at 23 °C; injection volume: 20 µL.

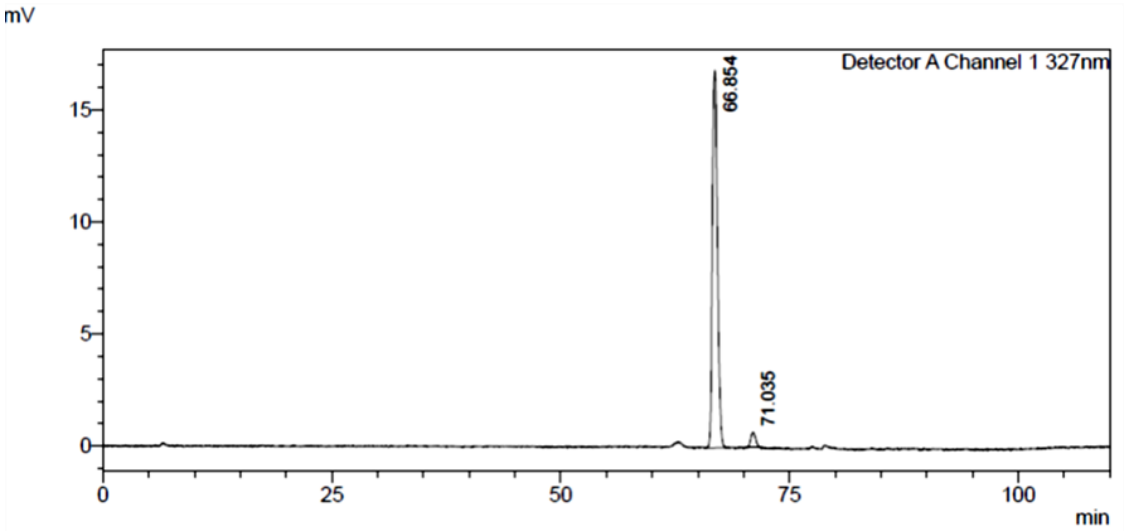

Figure 1. HPLC profile of AzoTP showing > 95% purity.

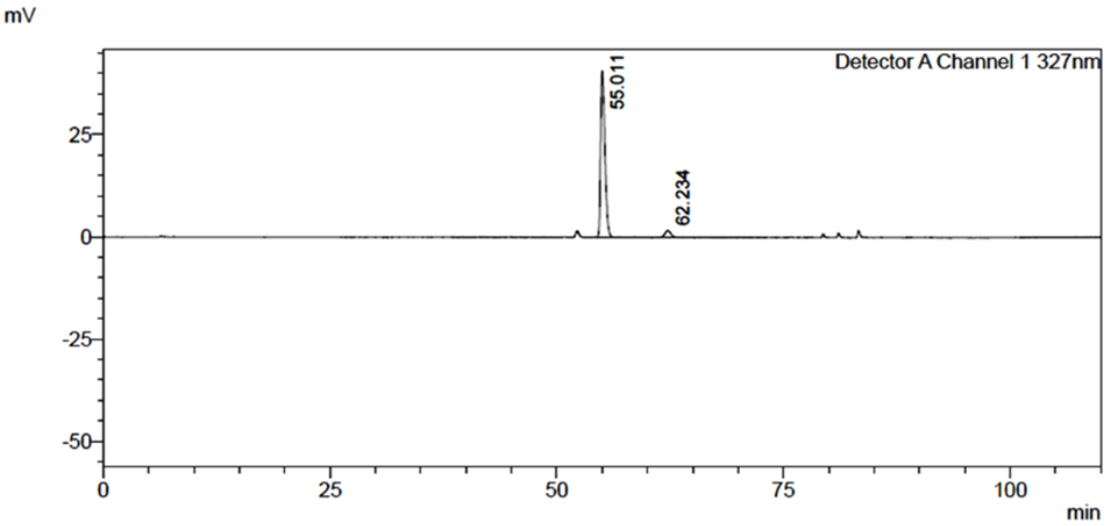

Figure 2. HPLC profile of AzoethoxyTP showing 95% purity**.**

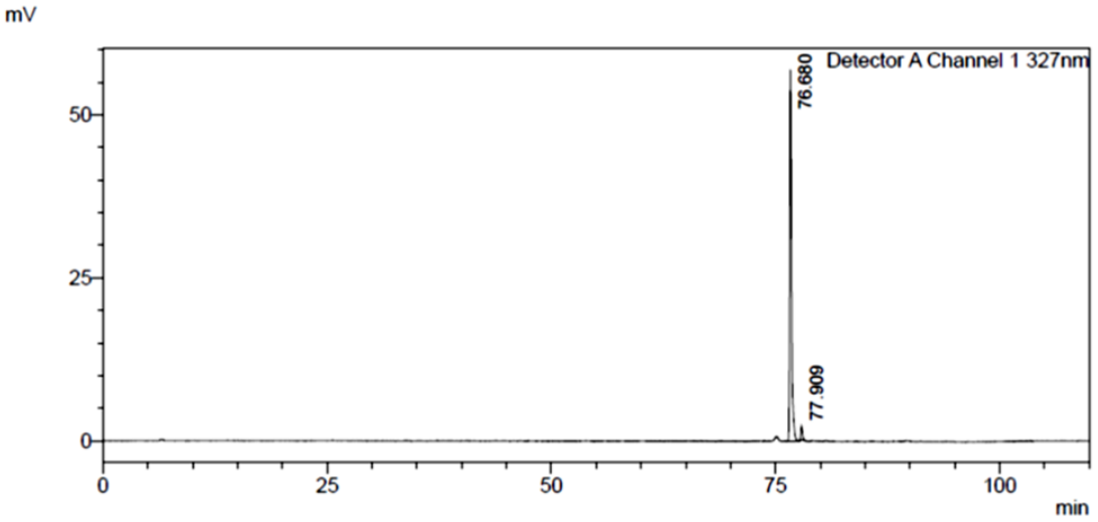

Figure 3. HPLC profile of DimethylazoTP showing > 95% purity.

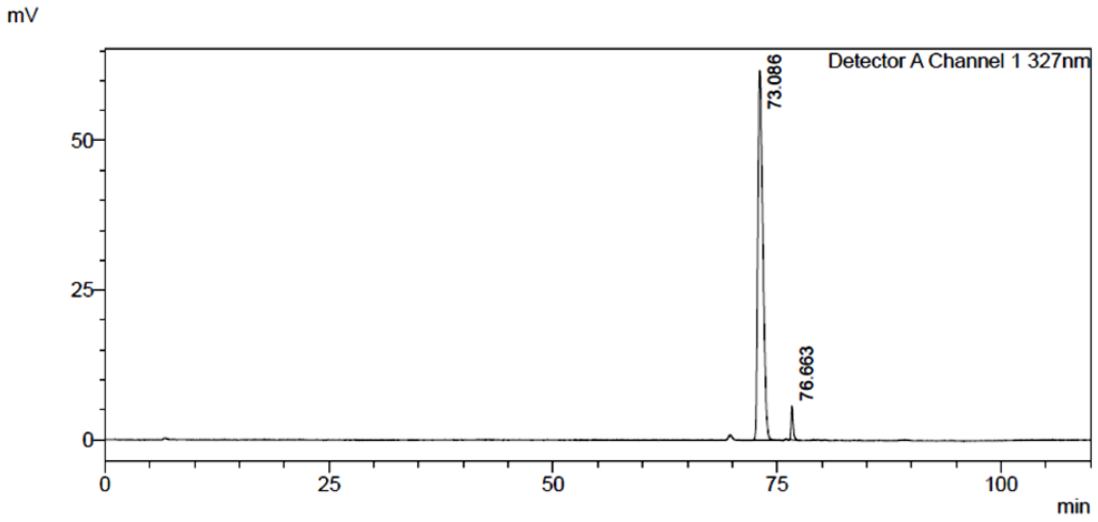

Figure 4. HPLC profile of AzoethylTP showing > 95% purity.

2.4.2 ESI - Mass spectra of AzoTP derivatives

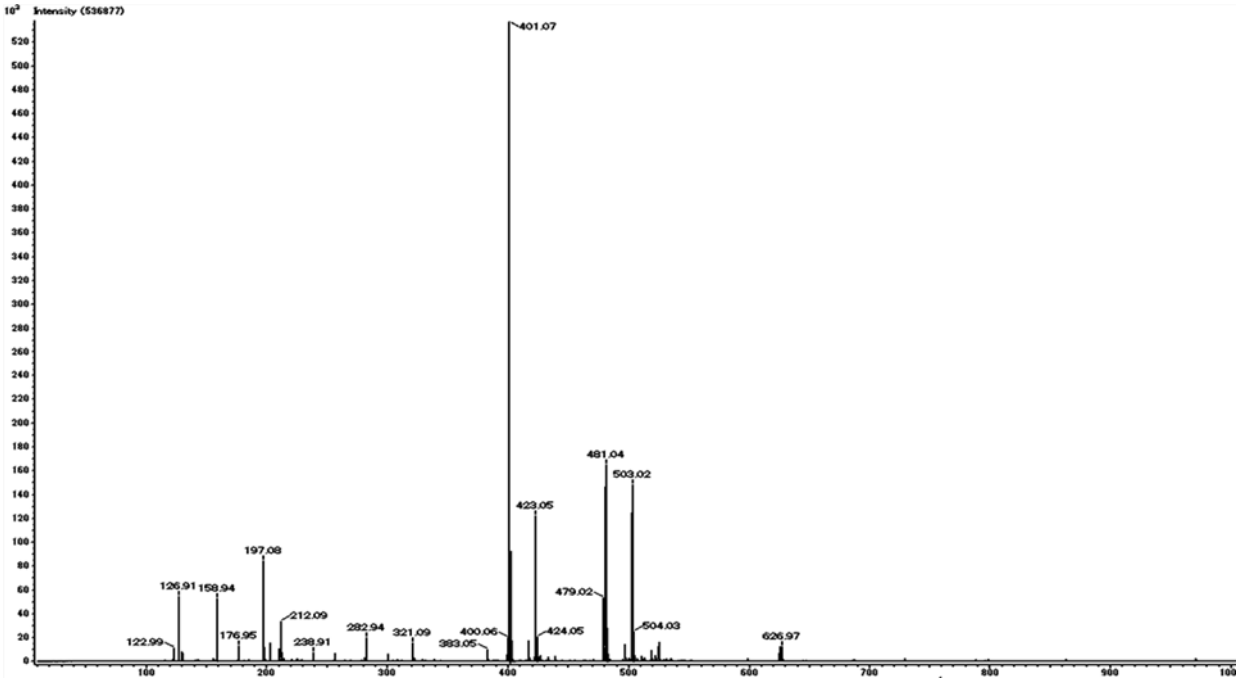

Figure 5. ESI^- mass spectrum of AzoethoxyTP, the peaks at *m/z* = 504.03, 503.02, 479.02 and 481.04 assigned to the $[M-H]^-$ ions of monosodium tetraprotonated, monosodium triprotonated, diprotonated and tetraprotonated AzoethoxyTP species respectively (calculated mass $[M-H]^-$ for these fragments $C_{14}H_{17}N_2O_{11}NaP_3$, $C_{14}H_{16}N_2O_{11}NaP_3$, $C_{14}H_{15}N_2O_{11}P_3$ and $C_{14}H_{17}N_2O_{11}P_3$ is 504.03, 503.02, 479.02 and 481.04 respectively). The peaks at *m/z* = 424.05, 423.05 and 401.07 assigned to $[M-H]^-$ ions of monosodium triprotonated, monosodium diprotonated and triprotonated AzoethoxyDP species respectively (calculated mass $[M-H]^-$ for these fragments $C_{14}H_{16}N_2O_8NaP_2$, $C_{14}H_{15}N_2O_8NaP_2$, $C_{14}H_{16}N_2O_8P_2$ is 424.05, 423.05 and 401.07 respectively).

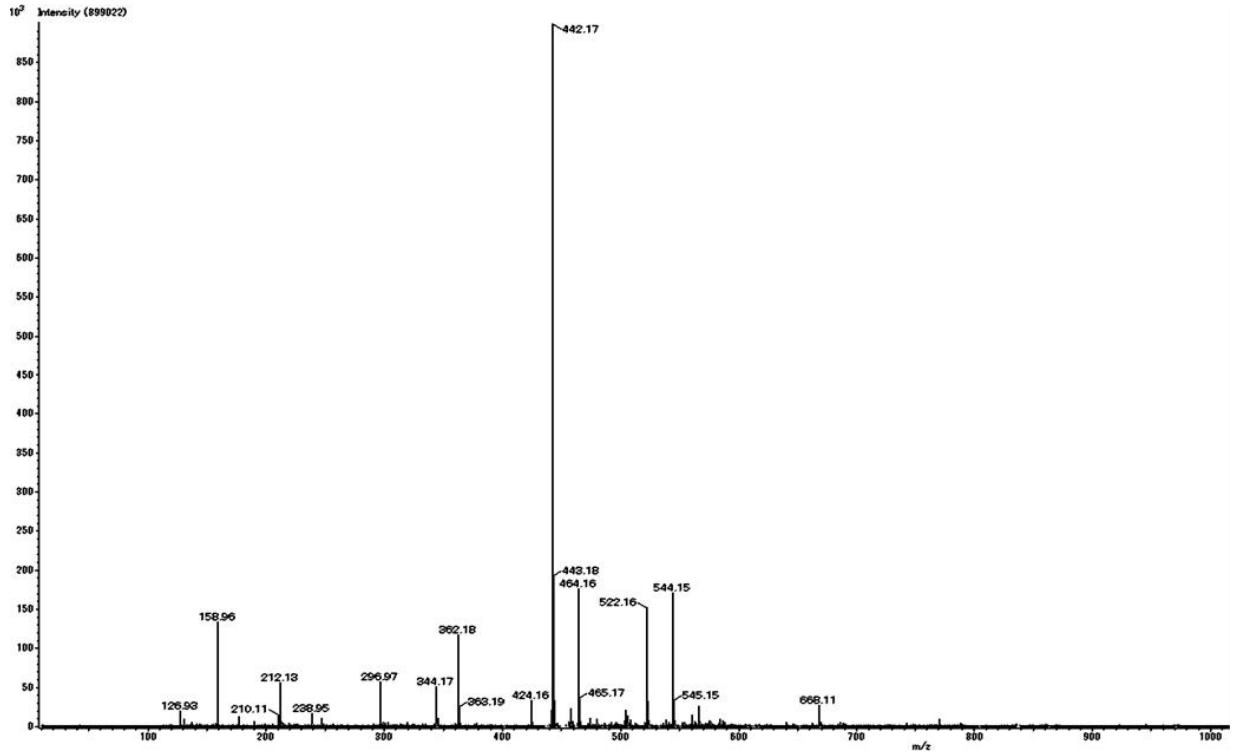

Figure 6. ESI mass spectrum of DimethylazoTP, the peaks at *m*/*z* = 544.15 and 522.16 can be assigned to the $[M-H]^-$ ions of monosodium triprotonated and tetra-protonated DimethylAzoTP species respectively (calculated mass $[M-H]^-$ for these fragments $C_{16}H_{18}N_3O_{11}NaP_3$ and $C_{16}H_{19}N_3O_{11}P_3$ is 544.15 and 522.16 respectively). The peaks at *m*/*z* = 464.16 and 442.17 can be assigned to the $[M-H]^-$ ions of monosodium triprotonated and tri-protonated DimethylAzoDP species respectively (calculated mass $[M-H]^-$ for these fragments $C_{16}H_{18}N_3O_8NaP_2$ and $C_{16}H_{19}N_3O_8P_2$ is 464.16 and 442.17 respectively).

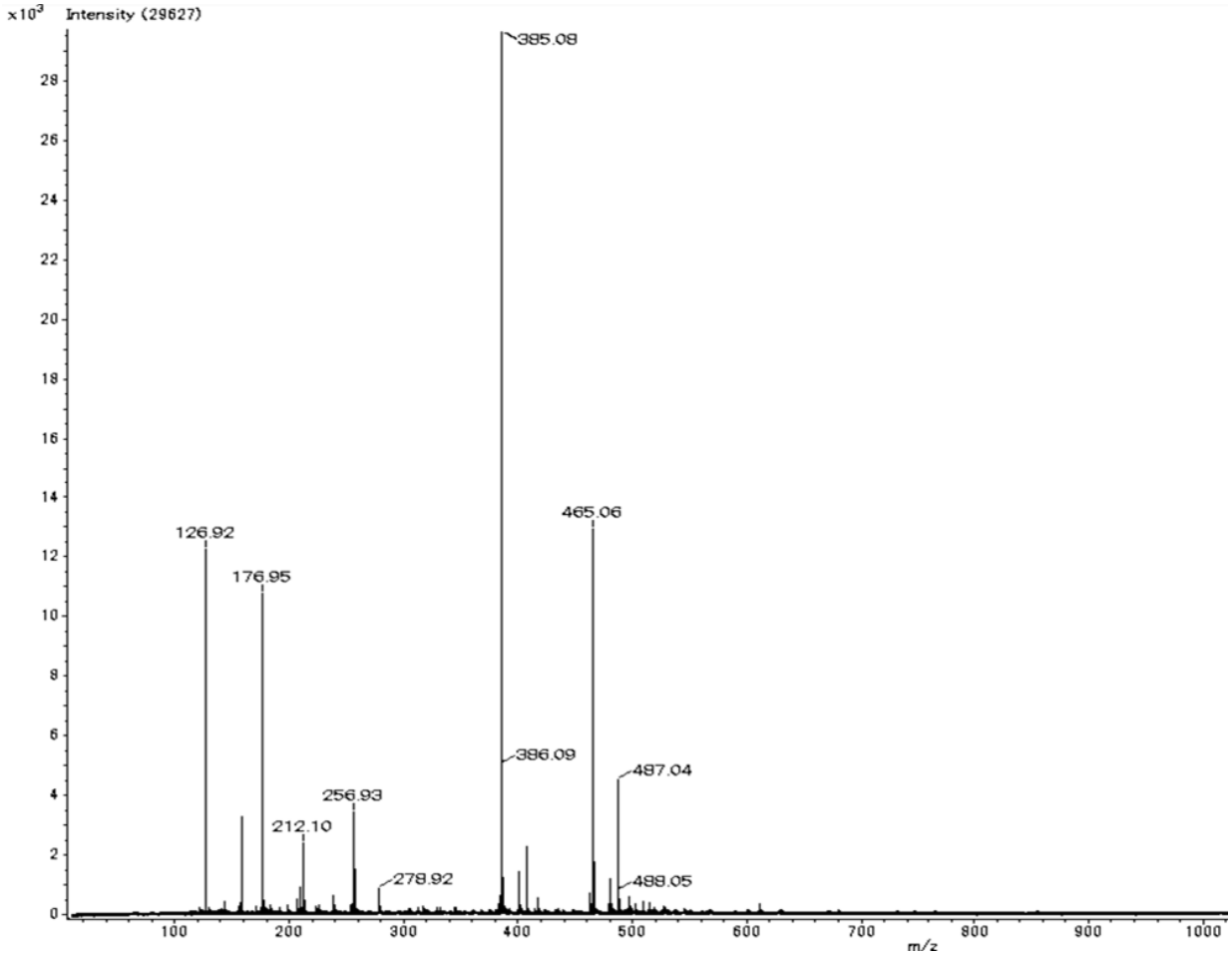

Figure 7. ESI mass spectrum of AzoethylTP, the peaks at *m*/*z* = 487.04, 465.06 and 385.08 can be assigned to the $[M-H]^-$ ions of monosodium triprotonated, tetra-protonated AzoethylTP and tri-protonated AzoethylDP species respectively (calculated mass $[M-H]^-$ for these fragments $C_{14}H_{16}N_2O_{10}NaP_3$, $C_{14}H_{17}N_2O_{10}P_3$, $C_{14}H_{16}N_2O_7P_2$ is 487.04, 465.06 and 385.08 respectively).

2.5 Protein extraction and purification

2.5.1 Preparation of skeletal muscle myosin from chicken

Myosin extraction was carried out at 4 °C

Solutions:

Extraction Buffer pH 6.5 (adjusted with K_2HPO_4)

0.3 M KCl

1 mM ATP (to be added just before using)

0.1 M KH_2PO_4

0.05 M K_2HPO_4

5 mM $MgCl_2$

20 mM EDTA (pH 8.0)

Stored at 4°C

Buffer A

2.85 M KCl

0.36 M KPi buffer (pH 6.5)

Stored at 4°C

KPi Buffer (1 liter)

pH 6.5

272 g of KH_2PO_4

348 g of K_2HPO_4

1. 50 g of fresh chicken muscle was weighed and cooled on ice.

2. Diced the muscle as fine as possible (27 g) and then added 3 volume of extraction buffer (81 mL).

3. Homogenized it by using polytron and stirred the suspension constantly for 10 min.

4. Centrifuged for 15 min at 12,000 rpm (23,000 X g).

5. Recovered the supernatant by filtering through gauze.

6. Measured the volume of the solution (70 mL) and diluted it to 14-fold with cold ddH_2O. The cold ddH_2O was let to flow very slowly into the beaker with stirring.

7. Incubated the suspension for 30 min in the cold room (4°C).

8. Pelleted the precipitated myosin by centrifugation at 7,000 rpm (8,000 X g) for 15 min.

9. Re-suspended the pellet in cold ddH_2O (the volume of suspension was 0.9 volume of muscle weight finally (24.3 mL)).

10. 3.2 mL of Buffer A (1/9 volume of the suspension) was added to dissolve myosin.

11. Centrifuged for 30 min at 18,000 rpm (39,000 g).

12. Recovered the supernatant by filtering with gauze.

13. Measured the volume of the solution (27.5 mL) and diluted it to 10-fold with cold ddH_2O (275 mL). The cold ddH_2O was let to flow very slowly into the beaker with stirring.

14. Pelleted the precipitated myosin by centrifugation at 12,000 rpm (23,000 X g) for 15 min.

15. Dissolved the pellet with 3 M KCl (16 mL final volume) making 0.5 M final concentration and centrifuge for 10 min at 12,000 rpm (23,000 X g) to remove the denatured aggregates.

16. Collected the supernatant and measured the protein concentration (Abs280: 0.53 for 1mg/ml myosin solution).

17. Measured the volume of supernatant (16 mL). Added same volume (16 mL) of cold glycerol and mixed slowly. This myosin solution was stored at -20°C, it can be stored for several months.

Yield = 385 mg.

2.5.2 Preparation of heavy meromyosin (HMM) from chicken skeletal myosin.

HMM was prepared from above explained previously prepared skeletal muscle myosin from chicken. The preparation was carried out at 4 °C.

Solutions:

Solution A 0.5 M KCl

10 mM KPi buffer (pH 6.5)

2 mM $MgCl_2$

Solution B 0.5 mg/ml α-Chymotrypsin in 0.001 N HCl

Solution C 0.1 M PMSF in 2-propanol

Solution D 20 mM KCl

10 mM KPi buffer (pH 6.5)

1. Diluted myosin stock solution (15 mL) stored in 0.25 M KCl and 50% glycerol by adding 5 volume of cold 0.3 mM $KHCO_3$ (75 mL) slowly with stirring.

2. Centrifuged for 10 min at 12,000 rpm (23,000 X g).

3. Dissolved the pellet with cold Solution A (9 mL) to make 20 mg/ml myosin solution.

4. Preincubated myosin solution at 25°C for 5 min.

5. Added 1 mL of α-Chymotrypsin (Solution B) so that to make the final concentration to 0.05 mg/ml and incubated at 25°C for 10 min.

6. Stopped the reaction by adding 20 µL of Solution C (PMSF) to a final concentration of 0.2 mM with stirring.

7. Dialyzed this solution against Solution D overnight at 4°C.

8. Centrifuged for 30 min at 18,000 rpm (50,000 g).

9. Recovered the supernatant (HMM fraction) and measured the protein concentration (Abs280: 0.63 for 1 mg/ml myosin solution).

10. Aliquoted the HMM solution and froze them in liq N_2 rapidly. This HMM solution can be stored for several years at -80°C.

Yield = 15 mg. (1.8 mg/mL)

2.5.3 Preparation of F-actin from sucrose powder

Actin filaments were prepared from the rabbit skeletal muscle actin stocked as sucrose powder. Preparation was carried out at 4 °C.

Solutions:

G-buffer 0.2 mM $CaCl_2$

0.2 mM ATP

1.4 mM β-mercaptoethanol

2 mM Tris-HCl (pH 8.0)

F-buffer 5 mM HEPES - KOH (pH 7.4)

25 mM KCl

1.4 mM β-mercaptoethanol

1. Dissolved the sucrose powder with 10 (v/w) of G-buffer (200 mg : 2 mL)

2. Dialyzed the actin solution against 500 ml of G-buffer for 4 hours.

3. Centrifuged for 10 min at 45,000 rpm (90,000 g).

4. Recovered the supernatant (2.4 mL) and added KCl (82.8 µL of 3 M) to make a final concentration of 0.1 M.

5. Incubated on ice for 30 min allowing for polymerization.

6. Dialyzed the solution against 300 ml of F-buffer and changed the buffer 2 times.

7. Recovered the solution and measured the protein concentration (Abs280: 1.1 for 1 mg/ml F-actin solution).

8. Thus obtained F-actin solution was stored on ice for 15 days. This couldn't be frozen.

Yield = 15 mg (6.9 mg/mL).

F-actin was labelled with phalloidin -CF^{TM} 633 dye conjugate.

2.5.4 SDS-PAGE (Porzio & Pearson method)

The purity of above prepared proteins was analyzed by SDS-PAGE.

Solutions

2X SDS-Loading Buffer	100 mM Tris-HCl (pH 6.8)
	4% SDS
	0.2% bromophenol blue (BPB)
	20% glycerol
	0.7 M β-mercaptoehtanol
Premix Solution	50% glycerol
	2.5 mM SDS
	2.5 mM EDTA
CBB solution	2.5 g Coomassie Brilliant Blue R250 (or G250) in 45% methanol, 10% acetic acid
De-staining solution	45% methanol, 10% acetic acid

Sample preparation:

Protein solution	20 µl
2X SDS-Loading Buffer	200 µl

Mixed well by pipetting and then incubated at 100°C for 3 min. Vortexed briefly and then did the flash spin.

Gel (10 % acrylamide)

Premix Solution	1.92 ml
25% acrylamide-bis (100:1)	3.89 ml
0.5 M Tris-1.5 M Gly (pH8.9)	1.60 ml
10% APS	125 µl
TEMED	9 µl
ddH_2O	456 µl
Total	8 ml

Running buffer

0.5 M Tris-1.5 M Gly (pH8.9)	20 ml
10 % SDS	2 ml
ddH_2O	178 ml
Total	200 ml

1. Loaded the sample on the well of gel (20 µl)

2. Applied a constant current 5 mA until all BPB dyes came into the gel.

3. Applied a constant current 20 mA until the BPB dyes came to the bottom of the gel.

4. Stopped electrophoresis and then soaked the gel in CBB solution for 30 min.

5. Soaked in the de-staining solution overnight.

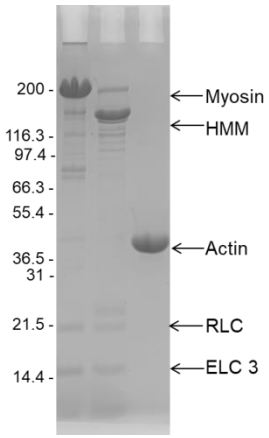

Figure 1. Protein purity determination; Samples of proteins were separated by electrophoresis in a SDS-PAGE system, and stained with Coomassie Blue. Arrows indicate the myosin heavy chain (approx. 200 kDa), RLC (approx. 20 kDa) and ELC (approx. 17 kDa), head domain of myosin-HMM (approx. 150 kDa) and actin (approx. 40 kDa).

2.6 Glycerinated muscle fiber preparation

Buffer: 137 mM NaCl + 2.7 mM KCl + 10 mM Na_2HPO_4 + 1.8 mM KH_2PO_4; pH 7.4

The chicken was killed, quickly skinned off and the skeletal muscle was extracted from the chicken breast. This muscle was then dissected into several muscle stipes of approximately 2 – 4 mm thickness. They were incubated at 0°C for 15 to 24 h in 50% glycerol/50% buffer solution. Then the solution was changed and the stripes were stored at - 20°C in the fresh solution. Fibres were used for up to 3 months.

2.7 Actin - myosin *in vitro* motility assay.

Flow cells: Two strips of double-sided adhesive tape were placed on a glass slide, ca. 3 mm apart, and an 18x18 mm cover slip coated with 0.1% of nitrocellulose in amyl acetate was placed on these strips providing a flow cell with working volume of 3-5 µL. The assay solutions were pipetted-in on one end and flown out from the other end of the flow path (between the two strips).

Buffers:

DTT-assay buffer

100 mM HEPES (pH 7.4) + 25 mM NaCl + 4 mM $MgCl_2$ + 1 mM EGTA + 10 mM DTT

BSA-DTT-assay buffer

100 mM HEPES (pH 7.4) + 25 mM NaCl + 4 mM $MgCl_2$ + 1 mM EGTA + 0.5 mg/mL BSA + 10 mM DTT.

ATP/AzoTP-assay buffer

100 mM HEPES (pH 7.4) + 25 mM NaCl + 4 mM $MgCl_2$ + 1 mM EGTA + 0.5 mg/mL BSA + 10 mM DTT + oxygen scavenger (20mM glucose + 20 μg/mL catalase + 0.1 mg/mL glucose oxidase) + ATP/AzoTP.

Procedure:

The HMM solution 3 μL (diluted with DTT-assay buffer, ca. 0.29 mg/mL) was perfused into flow cell and incubated for 2 minutes. Then flow cell was washed with 3 μL of BSA-DTT-assay buffer and F-actin solution 3 μL (diluted with BSA-DTT-assay buffer, ca. 2 μg/mL) was perfused. After 2 minutes of incubation, the flow cell was washed with 3 μL of BSA-DTT-assay buffer. Then 3 μL of ATP/AzoTP-assay buffer was perfused into the flow cell and the motility of actin filaments were observed under an inverted fluorescence microscope. The flow cell was irradiated with 365 nm and 436 nm light alternatingly and the motility of F-actin was recorded for 20 s with 2 frames/s after each irradiation. Gliding velocities were measured with ImageJ plugin MTrackJ.[37] Average of velocity of 10 filaments was determined in each experiment. All the assays were performed at 23.5 ^{o}C.

2.8 Kinesin - microtuble *in vitro* motility assay.

Buffers:

Kinesin buffer

80 mM PIPES (pH 7.5) + 1mM EGTA + 2 mM $MgSO_4$ + 0.5 mg/mL casein.

Microtubule buffer

80 mM PIPES (pH 7.5) + 1mM EGTA + 2 mM $MgSO_4$ + 10 μM taxol + 0.1 mg/mL casein.

Assay buffer

80 mM PIPES (pH 7.5) + 1mM EGTA + 2 mM $MgSO_4$ + 0.5 mg/mL casein + 10 μM taxol + oxygen scavenger (0.14M β-mercaptoethanol + 20 mM glucose + 20 μg/mL catalase + 0.1 mg/mL glucose oxidase) + ATP/AzoTP.

Procedure:

The kinesin solution 3 μL (diluted with kinesin buffer, ca. 100μg/mL) was perfused into flow cell and incubated for 3 min. Then the microtubule solution 3 μL (diluted with microtubule buffer, ca. 0.5μM) was perfused into the flow cell and incubated for 3 min. The flow cell was rinsed with 3 μL of microtubule buffer to remove unbound microtubules. After 1 min incubation, 3 μL of motility buffer with desired concentration of AzoTP was perfused into the flow cell and the motility of microtubules was monitored and recorded using fluorescence microscope. The flow cell was irradiated with 365 nm and 436 nm light alternatingly and the motility of microtubles was recorded for 40 s. Gliding velocities of microtuble were measured with ImageJ. Average of velocity of 10 microtubles was determined in each experiment. All the assays were performed at 23 ^{o}C.

2.9 Muscle fiber shortening experiments

Glycerol extracted chicken skeletal muscle stripes stored at -20^{o}C in 50% glycerol-buffer were transferred to a 20% glycerol-buffer solution 20 min before conducting the fibre shortening experiment and then transferred to the buffer solution without ATP/AzoTP 3 min before starting the experiment. The muscle stripe was teased into ~0.5 mm thick and 7 mm-8 mm long fibres which were then mounted on the glass slide and the buffer solution containing AzoTPs (4 µL) was added. The changes in the length were observed by unaided eyes and analysed the change in length by recording the video for shortening process using a Canon digital camera. The length change vs time was measured by dividing the net change in the length of the fibre with respect to its initial length at a time interval by the initial length ($L_{(t=0)}$-$L_{(t)}$ / $L_{(t=0)}$). For the photo-regulation experiments, the muscle fibres mounted on the slide were directly irradiated with 510 nm (LED) light after adding the buffer solution containing *cis*-rich state AzoTP substrates.

3. RESULTS AND DISCUSSION

3.1 Synthesis and photoisomerization of AzoTP derivatives

The derivatives of AzoTP were synthesized by modifying the bridging group between azobenzene and triphosphate and by substitution on azobenzene moiety of previously reported parent AzoTP (**1**). Substituting the amide linkage with ether and ethyl linkage resulted in AzoethoxyTP (**2**) and AzoethylTP (**4**) respectively, while the substitution of methyl groups at *meta* and *para* on azobenzene moiety resulted in DimethylAzoTP (**3**) [Figure1a)]. These modifications in the parent AzoTP were done to probe the critical significance of the amide linkage in functioning of AzoTP as an energy molecule and for exploring the possibility of a further efficient azobenzene based photochromic non-nucleoside triphosphate. The reversible photoisomerization of these AzoTPs was confirmed by consecutive irradiation with 365 nm UV light and 436 nm visible light (Figure 2). At UV photo stationary state (PSS) the AzoTPs attain their *cis*-rich state which is reversed at visible PSS resulting in thermodynamically stable *trans*-rich state. Our previous study of **1** in kinesin-microtuble motile system suggested that *trans* isomer of **1** was an efficient energy molecule that triggered the faster velocity of microtubules by driving kinesin motor whereas the *cis* isomer was inefficient to drive kinesin [Figure1b)]. Table 1 shows the ratio of *cis:trans* isomers of **1**, **2**, **3** and **4** at PSS induced by 365 nm and 436 nm light irradiation, determined by H^1NMR (Figure 3a-c). The thermal isomerization from *cis* to *trans* was evaluated by observing the changes in absorption spectra when kept in dark at room temperature. About 2% of *trans* isomer was recovered after 3h dismissing the possibility of thermal-back reactions during our experiments.

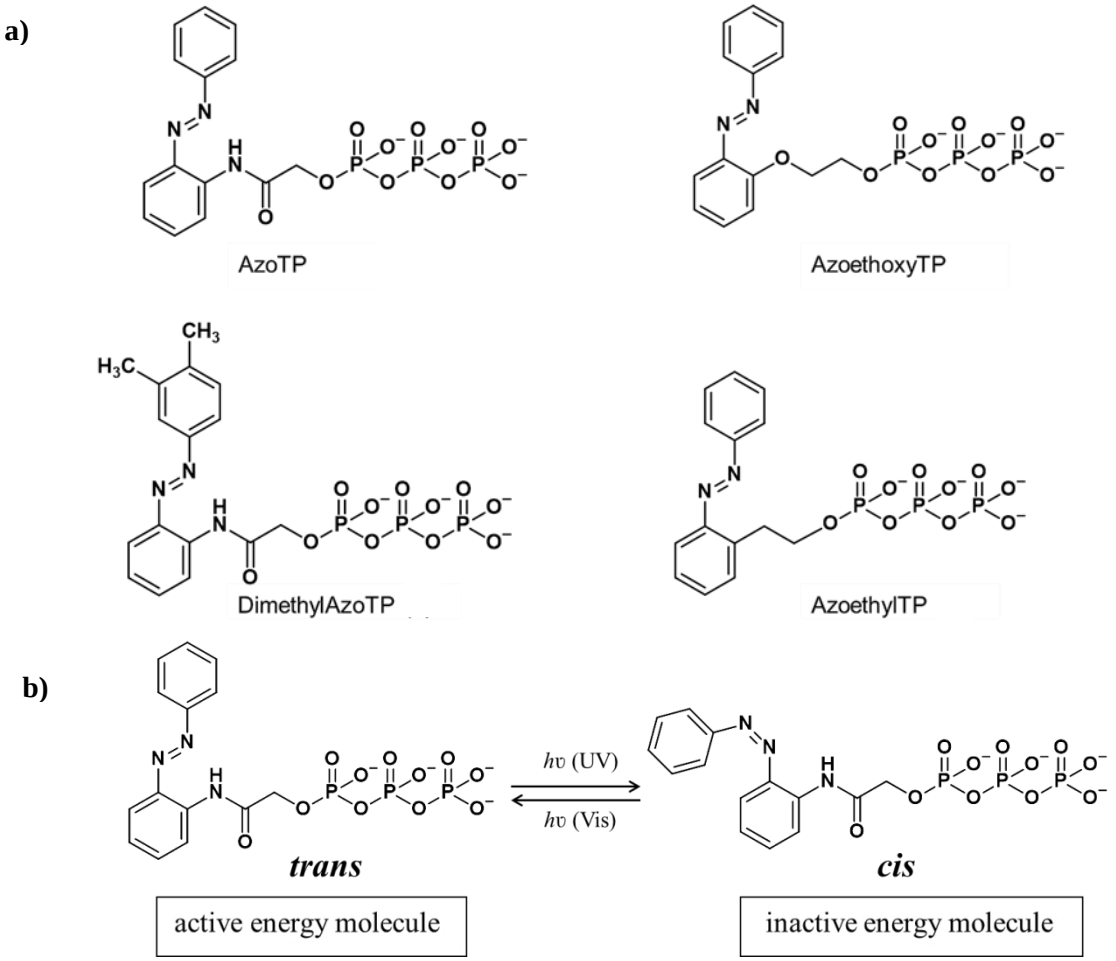

Figure 1. a) Structures of azobenzene based non-nucleoside triphosphates - AzoTP, AzoethoxyTP, DimethylAzoTP and AzoethylTP. b) Reversible photo-isomerization of AzoTP.

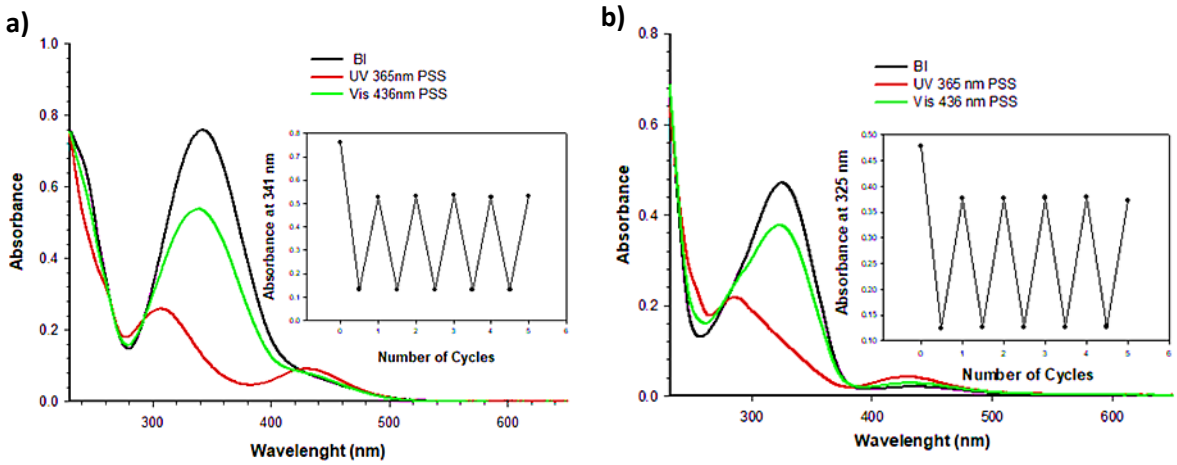

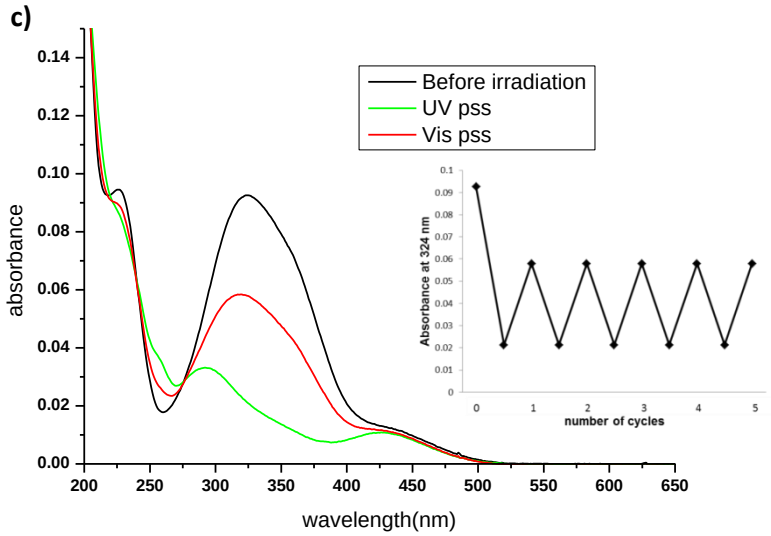

Figure 2. UV-Vis absorption spectra of AzoTP molecules **a)**DimethylAzoTP, **b)** AzoethylTP in BRB-80 buffer solution at 25 °C; before irradiation (black line), UV PSS (red line), Vis PSS (green line) and **c)** AzoethoxyTP in water at 25%. Insets show the absorbance changes a) at 341 nm, b) at 325 nm and c) at 324 nm after the alternate irradiations of 365 and 436 nm for 5 cycles.

Non-nucleoside triphosphate	UV PSS		Visible PSS	
	cis	*trans*	*cis*	*trans*
AzoTP	92%	8%	38%	62%
AzoethoxyTP	93%	7%	50%	50%
DimethylAzoTP	93%	7%	35%	65%
AzoethylTP	87%	13%	25%	75%

Table 1. Ratio of *cis* and *trans* isomers at UV and Visible photo stationary state (PSS).

a)

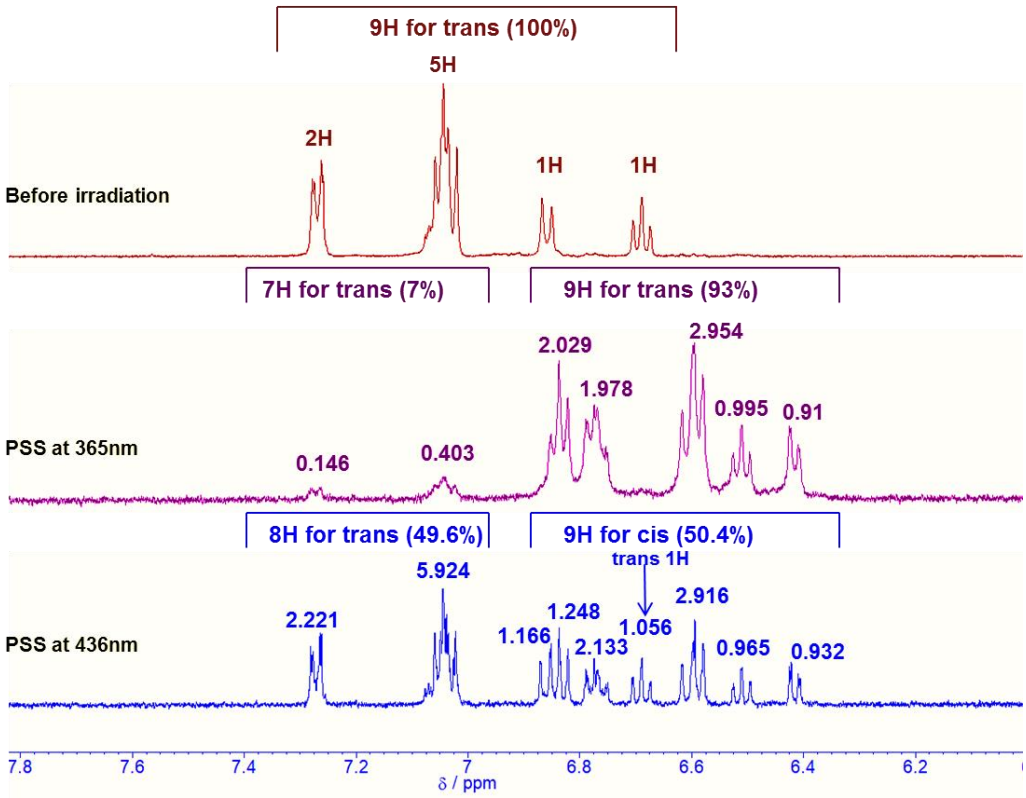
9H for trans (100%)
5H
2H
1H
1H
Before irradiation
7H for trans (7%)
9H for trans (93%)
2.029
2.954
1.978
0.995
0.91
PSS at 365nm
0.146
0.403
8H for trans (49.6%)
9H for cis (50.4%)
trans 1H
5.924
2.916
2.221
1.248
1.056
1.166
2.133
0.965
0.932
PSS at 436nm
7.8
7.6
7.4
7.2
7
6.8
6.6
6.4
6.2
δ / ppm

b)

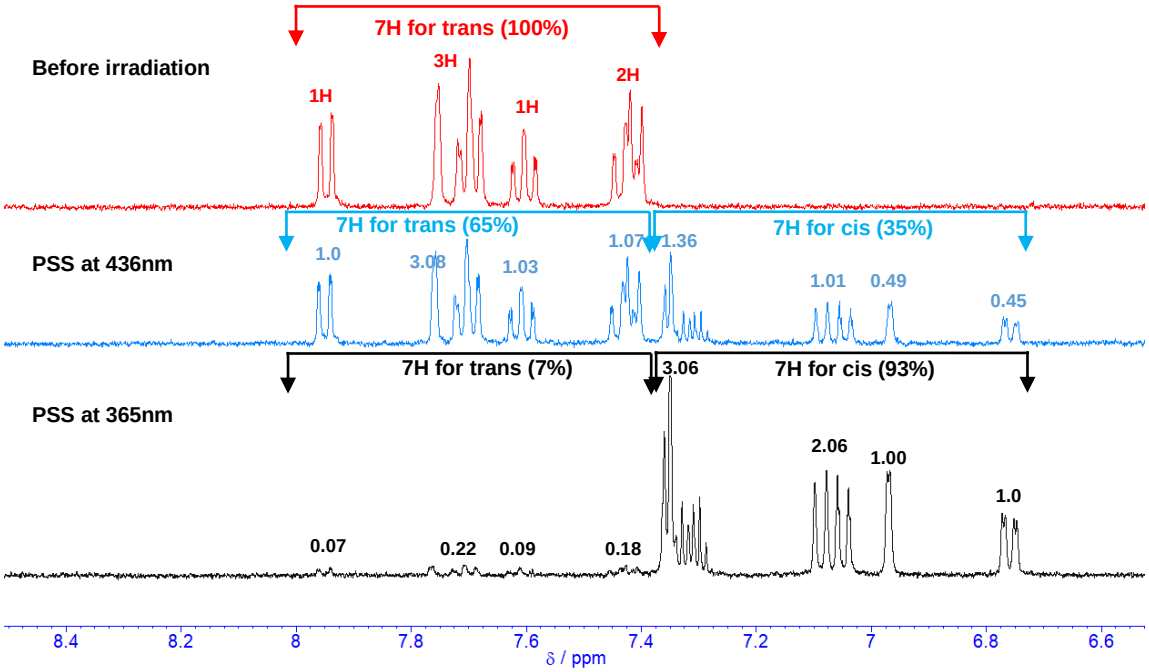
7H for trans (100%)
Before irradiation
1H
3H
1H
2H
7H for trans (65%)
7H for cis (35%)
PSS at 436nm
1.0
3.08
1.03
1.07
1.36
1.01
0.49
0.45
7H for trans (7%)
3.06
7H for cis (93%)
PSS at 365nm
2.06
1.00
1.0
0.07
0.22
0.09
0.18
8.4
8.2
8
7.8
7.6
7.4
7.2
7
6.8
6.6
δ / ppm

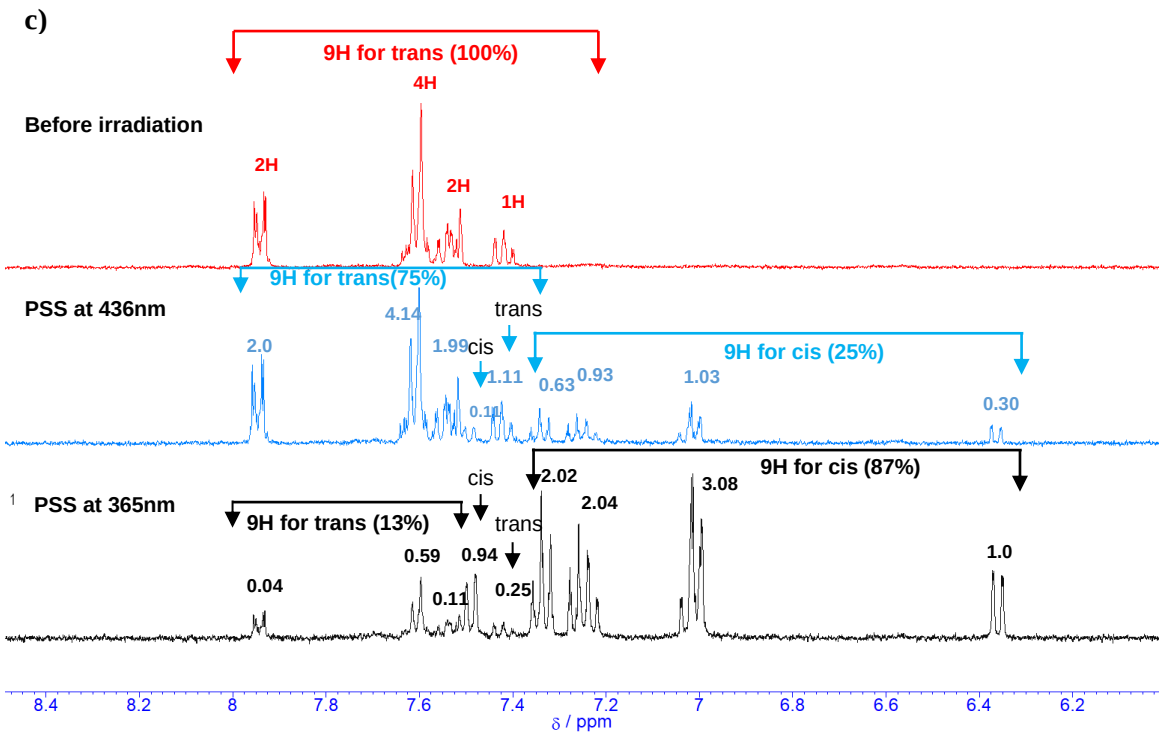

Figure 3. ^{1}H NMR spectra (400 MHz, D_2O) showing *trans* and *cis* isomer ratio of a) AzoethoxyTP, b) DimethylazoTP and c) AzoethylTP before irradiation, after UV PSS and Visible PSS.

3.2 Reversible photo-control of *in-vitro* motility of myosin-actin motile system

To assess the generalizability of AzoTP to drive and control the cytoskeletal motor systems, we employed **1** and also its derivatives AzoethoxyTP, DimethylazoTP and AzoethylTP in myosin-actin motile system as differing from our previously reported kinesin-microtuble system. HMM (heavy meromyosin) is a soluble fragment of myosin consisting of two heads (containing nucleotide binding site and actin binding site) and a part of myosin rod; hence it was used as an ATPase motor in our *in-vitro* motility assay experiments. All the four azoTP molecules tested, served as substrates for myosin by driving HMM induced gliding motility of F-actin on HMM immobilized glass surface, of which AzoTP and AzoethoxyTP functioned at

concentrations as low as 10 µM. The average velocity of F-actin triggered by AzoTP, AzoethoxyTP, DimethylazoTP and AzoethylTP are 1.25 µm/s, 1.50 µm/s, 1.24 µm/s and 0.73 µm/s respectively at saturated concentration of 0.5 mM for AzoTP, DimethylazoTP and AzoethylTP and 0.25 mM for AzoethoxyTP. Photo-induced reversible control of the gliding velocity of F-actin prompted by the photo-isomerization of AzoTPs was observed as the flow cell of motility solution was irradiated with 365 nm and 436 nm light alternatingly to the PSS. The velocity decreased remarkably after irradiation with 365 nm light for 5 s corresponding to *cis*-rich state, the subsequent irradiation with 436 nm for 20 s recovered the velocity, comparable to that of initial velocity before irradiation. This phenomenon of reversible switching between the faster and slower velocity could be repeated over many cycles as represented in Figure 4a-d. We carried out *in-situ* photo-regulation of F-actin velocity by repeated alternating irradiation of flow cell with 365 nm UV and 510 nm visible light for 3 s and 5 s respectively captured in the 5 min long video. Speeding actin filaments slowed down following the UV irradiation at a time interval and these slowly moving filaments recovered their speed after irradiation with 510 nm light. The magnitude of distance treaded by selected actin filaments facilitated by consecutive UV and Visible light irradiation at different time intervals is depicted in Figure 5. The change in velocity between the two photoisomerized states of AzoTP molecules is 54%, 79%, 81%, 80% for AzoTP, AzoethoxyTP, DimethylazoTP and AzoethylTP respectively at saturated concentrations. However, at 0.1mM concentration the magnitude of switching is higher for all AzoTPs as the difference in velocity is about 87 – 90%.

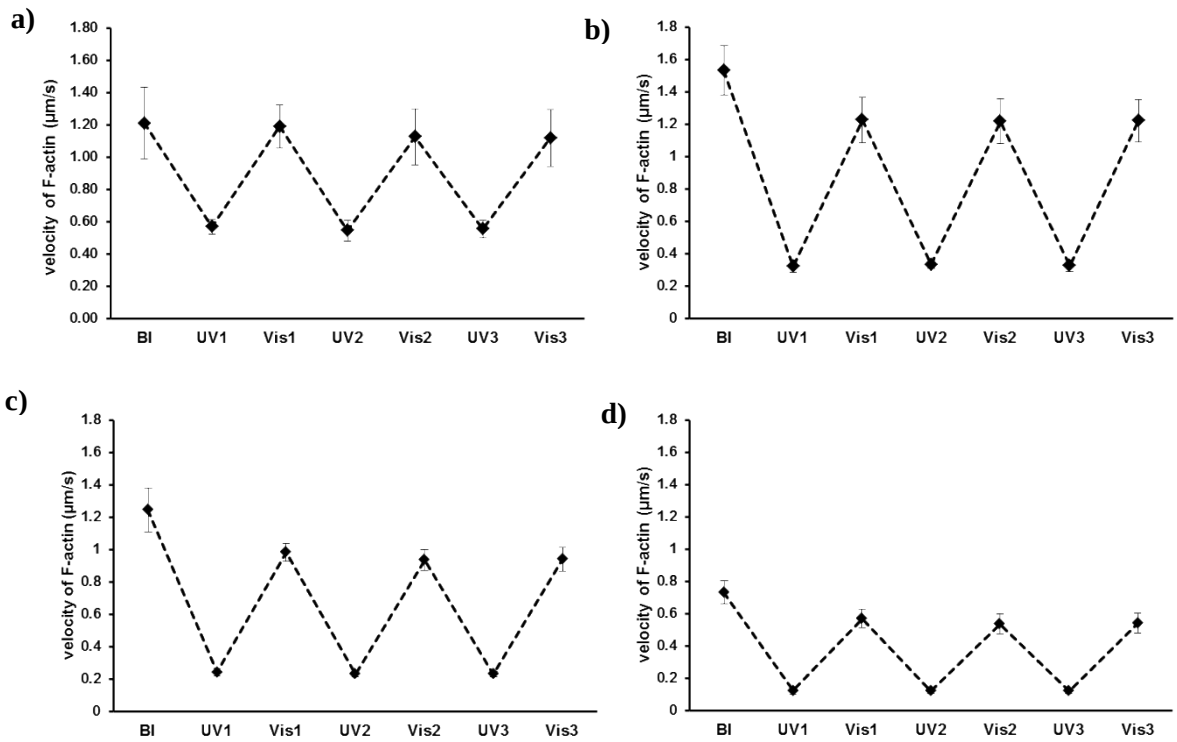

Figure 4. Repeated complete and reversible photoregulation of F-actin gliding velocity induced by a) AzoTP, b) AzoethoxyTP, b) DimethylazoTP and d) AzoethylTP at saturated concentration of 0.5, 0.25, 0.5 and 0.5 mM respectively. (BI: before irradiation; UV: after irradiation with 365 nm light; Vis: after irradiation with 436 nm light). Error bars: standard deviation for 10 actin filaments.

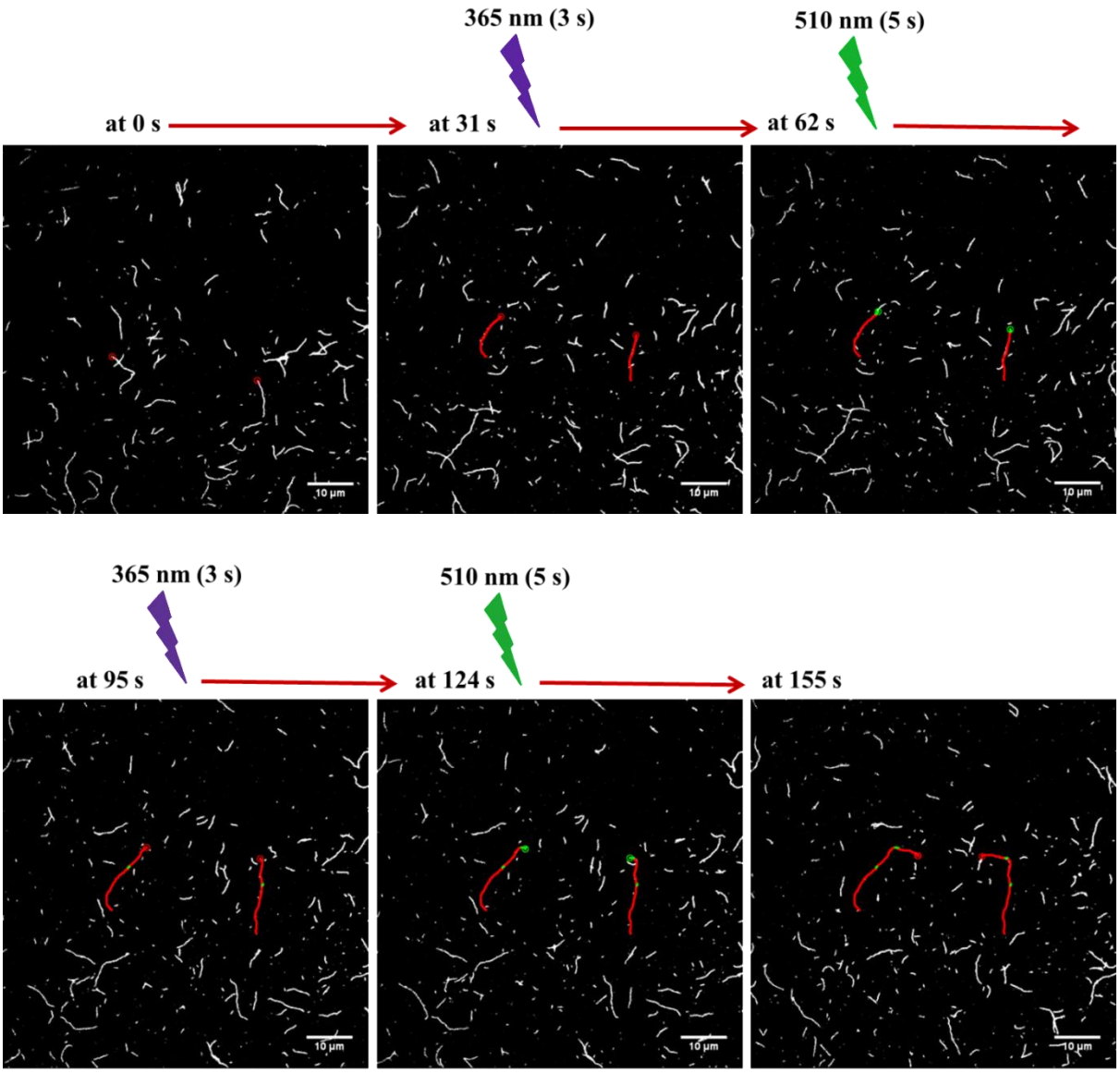

Figure 5. Fluorescence images of F-actin motility driven by *trans* and *cis* state of AzoTP (40 µM) by *in-situ* photo-regulation experiment with alternating irradiation at 365 nm (3 s) and 510 nm (5 s). The distance moved by two actin filaments is indicated in lines by tracking the path of filament heads; red circles denote the position of actin filament heads before irradiation (*trans* state), green and red lines denote the distance treaded by F- actin after UV (365 nm) and Vis (510 nm) irradiations respectively.

The gliding velocities fuelled by AzoTPs in their *trans* state (black solid circles) and *cis*-rich state (blue solid circles) with respect to the range of concentrations are shown in Figure 6. Concentration dependent velocity of actin filaments obeys the Michaelis-Menten equation and the obtained apparent K_m (K_{app}) values indicate that the apparent binding affinity of AzoTP for myosin ($1/ K_{app}$ = 9.9 mM^{-1}) is twenty five times higher than that for kinesin motor ($1/ K_{app}$ = 0.4 mM^{-1}) (as obtained in our previous work). The maximum gliding velocity (V_{max}) of F-actin induced by AzoTP, AzoethoxyTP, DimethylazoTP and AzoethylTP are 1.5 µm/s, 1.9 µm/s, 1.7 µm/s and 1.0 µm/s respectively, which are 53%, 68%, 59% and 35% of that of ATP (V_{max} = 2.9 µm/s) at saturated concentration. Our previous report on AzoTP explained that the microtubule velocity driven by *cis*-rich state of AzoTP is due to the remaining *trans* at *cis*-rich PSS, which corresponded to 8%. In our current study too we plotted a theoretical curve corresponding to remaining *trans* of all the four AzoTP molecules at their respective *cis*-rich PSS to validate this explanation. Figure 6. shows the Michaelis-Menten plot for concentration dependent velocity of all four AzoTPs and theoretical curve (red lines) for remaining *trans* amounting for 8%, 7%, 7% and 13% (table 1) in *cis*-rich state of AzoTP, AzoethoxyTP, DimethylazoTP and AzoethylTP respectively. These observations insinuate that AzoTPs in their *cis* state intrinsically have no ability to function as energy molecules to drive the motor proteins.

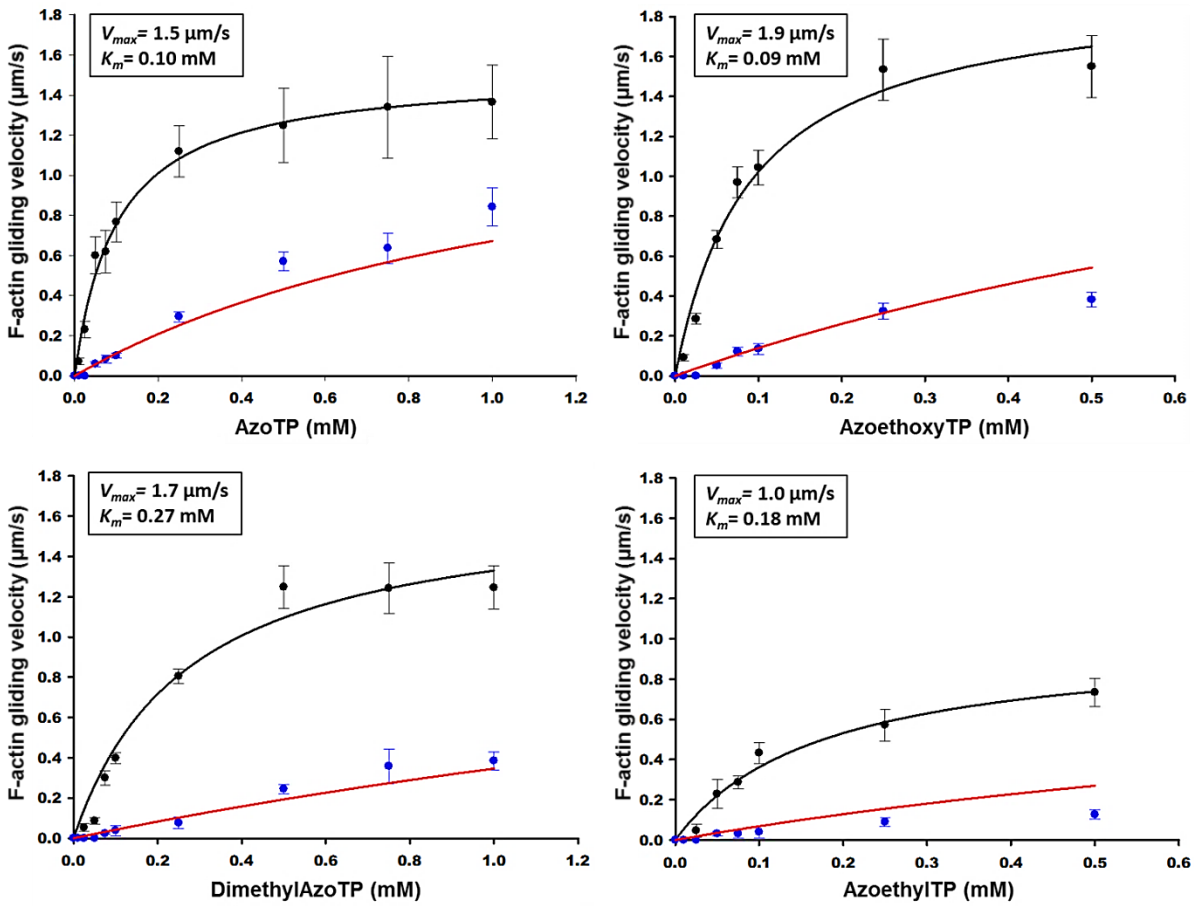

Figure 6. Gliding velocity of actin filaments as a function of AzoTPs concentration. (Black solid circles: velocities before irradiation; black line: curve fitted using Michaelis–Menten equation; Blue circles: velocities after irradiating at 365 nm; red line: theoretical curve derived from the black line for remaining *trans* in the *cis*-rich state.) Error bars: standard deviations for 10 actin filaments.

Although the K_{app} of AzoTP and AzoethoxyTP is almost threefold less than DimethylazoTP, the V_{max} of these three AzoTPs is comparable, since all three K_{app} were in submillimolar range. However, AzoethylTP has considerably lower V_{max}, though its K_{app} is in the same range as that of AzoTP, AzoethoxyTP and DimethylazoTP. These results imply that the substrates AzoTP and AzoethoxyTP bind to the myosin motor with higher affinity than that of DimethylazoTP and

AzoethylTP. Structural studies of chicken skeletal myosin subfragment 1 revealed that the nucleotide binding pocket is formed by the residues from the N-terminal, central, and C-terminal sections of myosin motor head domain.[27,28] The adenine binding pocket is formed by amino acid residues Phe[129]-Tyr[135] and Glu[187]-Lys[191] contributed by the N-terminal segment as seen in the X-ray structural studies of *Dictyostelium discoideum* myosin II complex (S1dC.MgADP.BeF_x).[29] Despite the presence of several water molecules with the potentiality for hydrogen bonding, very few specific interactions were seen between the adenine base and myosin heavy chain except the hydrogen bond between N6 of adenine and sidechain of Tyr[135]. This is in line with the observations that myosin utilizes a wide range of nucleotides and organic triphosphates,[30,31] thus substantiating the functionality of our AzoTP molecules as substrates for myosin. Also the ribose moiety which bridges the adenine and triphosphate moieties forms very few interactions with the protein, enabling the myosin to utilize nucleotides and organic triphosphates with ribose ring replaced by variety of functional groups. However, ribose ring oxygen, O4' forms a hydrogen bond with Asn[127] sidechain.[29] Comparing the chemical structures of our AzoTP molecules with that of ATP suggests that the linker groups (ether, amide, ethyl) might fulfil the role of ribose and azobenzene takes adenine's place. This presumption provides an insight into the varied binding affinity of our four AzoTP substrates as well as their *cis* and *trans* isomers. Higher binding affinity of AzoethoxyTP ($1/K_{app}$ = 11.0 mM^{-1}) could be attributed to the ether group bridging the triphosphate moiety and azobenzene, where the oxygen of ether forms a hydrogen bond with the side chain of Asn[127], analogous to the ribose oxygen of ATP.[29] Similarly the carbonyl oxygen of amide group in AzoTP could participate in the

hydrogen bonding by acting as a hydrogen acceptor. Absence of any potential hydrogen bond forming atoms in the bridging ethyl group elicits the lower binding affinity ($1/K_{app}$= 5.7 mM^{-1}) in AzoethylTP than AzoTP and AzoethoxyTP. Although there is carbonyl oxygen in DimethylazoTP with the potentiality for hydrogen bond formation, yet the binding affinity ($1/K_{app}$ = 3.7 mM^{-1}) is almost three fold lower than AzoTP and AzoethoxyTP. We assume this weaker binding affinity is resulted by the bulkiness of the substrate due to the presence of two methyl substituents on azobenzene moiety which might sterically interfere in the binding of substrate and myosin. AzoTPs in their *cis* state show no intrinsic ability as substrates for myosin unlike the active *trans* state. It is well established that the isomerization of azobenzene from *trans* to *cis* changes the geometry from flat to bent or round shape resulting in bulkiness. We surmise that the inability of *cis* isomer to bind in the nucleotide binding pocket could be ascribed to its bulkiness. In addition the adenine binding site is relatively hydrophobic[32,33] thus the hydrophilic *cis* isomer isn't favoured.

3.3 Photo-control of *in-vitro* motility of kinesin-microtuble motile system by AzoethoxyTP

Photoresponsive energy molecule AzoethoxyTP was found to be of the higher efficiency in the myosin-actin motor system amongst the newly synthesized AzoTP derivatives. Inorder to analyse its efficiency in driving and photoswitching the kinesin motor function, AzoethoxyTP was employed in the *in-vitro* motility assay of kinesin-microtuble system. AzoTP derivative AzoethoxyTP drives the kinesin motor albeit with lower efficiency than that of myosin. The average gliding velocity of

microtubules triggered by AzoethoxyTP was 0.1 μm/s, which is about 17% of the velocity obtained by ATP. Contrary to the myosin-actin system, AzoethoxyTP was unable to photoswitch the gliding velocity of microtubules by alternating irradiation with 365 nm and 436 nm light efficiently. However, a negligibly small difference between the *cis* and *trans* isomer triggered gliding velocity was observed (Figure 7). These results indicate that AzoethoxyTP's binding affinity for kinesin motor is lower than that for myosin. Both the *trans* and *cis* isomers bind to the kinesin motor with the comparable affinity.

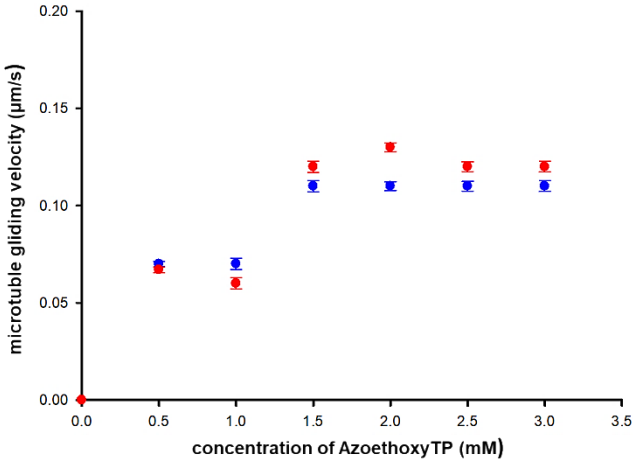

Figure 7. Gliding velocity of microtubles with respect to the concentration of AzoethoxyTP. Blue cirlcles: velocity before irradiation (*trans* state), red circles: velocity after 365nm irradiation (*cis* state). Error bars: standard deviations for 10 actin filaments.

3.4 Photo induced regulation of glycerinated skeletal muscle fibre system

As an approach to probe the efficiency of AzoTPs at macroscopic level to drive and control the motile functions, we conducted the simple glycerinated muscle fibre shortening experiments where the extent of shortening was assessed by unaided eyes.

The fibres used were of ~ 0.5 mm thickness and 7- 8 mm in length. First we tested our parent AzoTP molecule for macroscopic studies. AzoTP in its *trans* state induced the shortening of muscle fibre accounting for 40 – 45% shortening of muscle fibre's initial length. Pre-generated *cis* isomer of AzoTP didn't induce any significant shortening, thus affirming the poor activity of AzoTP in its *cis*-form as evidenced in our molecular *in-vitro* motility experiments (Figure 8a). When the *cis* isomer infused muscle fibre was irradiated with 510 nm light for 10 s, remarkable shortening of about 40% of its initial length was observed, thus confirming the efficiency of AzoTP to drive and photocontrol the myosin motor function in the macroscopic system (Figure 8b). To corroborate that the shortening was resulted by the photoisomerization of AzoTP and not by the thermal energy of illumination, we irradiated the muscle fibre infused in buffer solution without AzoTP at 510 nm, which exhibited no shortening (Figure 8c).

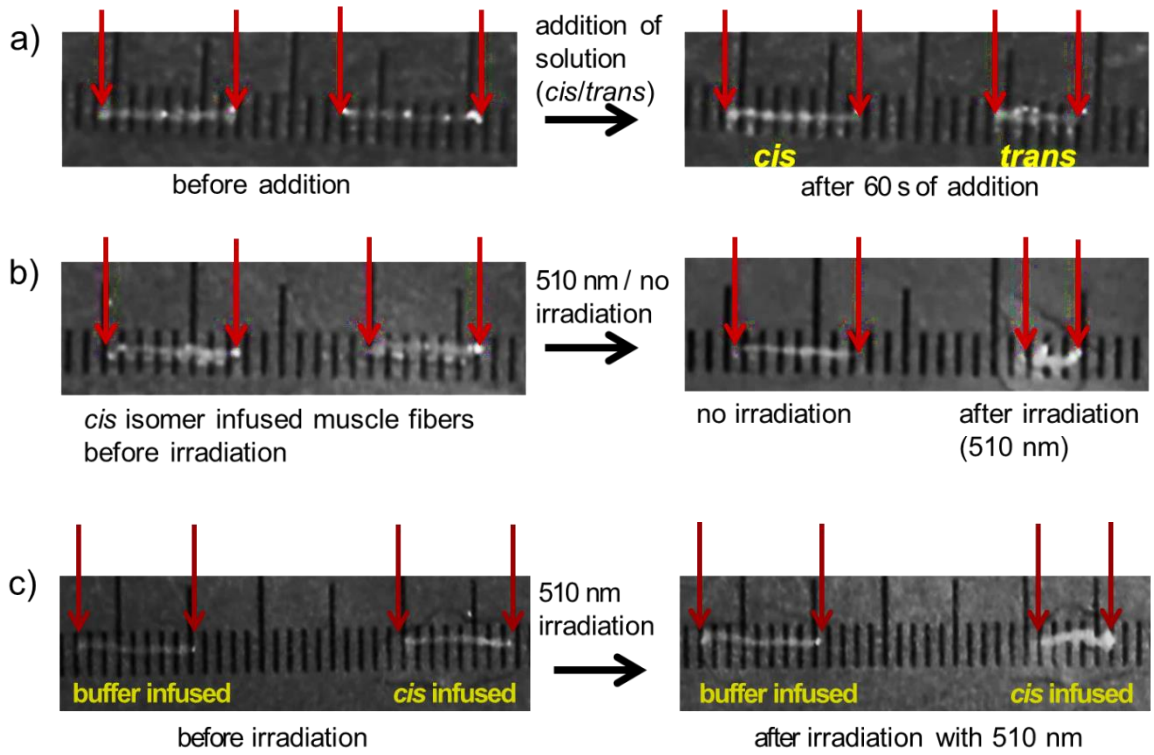

Figure 8. Non-nucleoside triphosphate AzoTP induces and photo-controls the shortening of glycerinated muscle fibre. a) buffer solution containing *trans*- AzoTP (3 mM) induced shortening while *cis*- AzoTP had no significant effect on shortening; b) *cis*- AzoTP infused muscle fibre shortened after irradiation with 510 nm light, no significant change in length in the non-irradiated fibre; c) muscle fibre infused with only buffer solution (without AzoTP) didn't shorten after irradiating with 510 nm whilst the buffer containing *cis*- AzoTP shortened after irradiating with 510 nm. Red arrows point at the two edges of the fibre. The scale seen in the photographs is 1 mm.

The ability of all three newly synthesized AzoTPs to initiate and photo-control the shortening was investigated. Figure 9. represents the percentage change in muscle fibre length with respect to time, induced by all the four AzoTPs at 3 mM (total). Shortening of muscle fibre with respect to time increases with the order of AzoTP~ AzoethoxyTP > DimethylazoTP > AzoethylTP, where the substrates AzoTP and AzoethoxyTP induce the shortening swiftly with evidently larger magnitude of length change than DimethylazoTP and AzoethylTP over the time range. Similar to AzoTP, the *cis*-form of energy molecules AzoethoxyTP, DimethylazoTP and AzoethylTP was unable to induce any significant shortening and the 510 nm light irradiation of *cis* infused muscle fibres induces the shortening except AzoethylTP. Experiments involving the AzoTP concentration dependent shortening rate showed that there is no significant change in muscle length below 0.5 mM of *trans*-AzoTP (Figure 10). This explains the no significant shortening induced by *cis*-rich state of AzoTP at 3 mM (total) despite the presence of expected 8% (0.25 mM) of remained *trans*. The order

of performance of four AzoTP substrates (AzoTP~ AzoethoxyTP > DimethylazoTP > AzoethylTP) in macroscopic system is consistent with the K_{app} values obtained by the molecular level studies. Unlike the molecular *in-vitro* motility system, the glycerinated muscle fibre system involves the ordered array of myofibrils which could furnish the steric hindrance, but the AzoTPs efficiently replicated the photo-regulation of motor function in the glycerinated muscle fibre as well. AzoTP energy molecules photo-regulate the muscle fibre shortening by photoisomerizing to active *trans* state from inactive *cis* state locally in the muscle fibre by direct photo-irradiation.

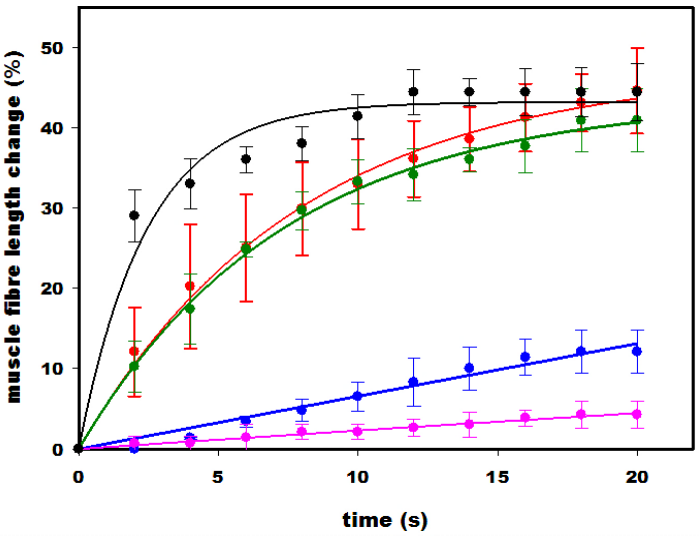

Figure 9. Muscle fibre length change ($L_{(t=0)}$ - $L_{(t)}$ / $L_{(t=0)}$) with respect to the time for AzoTPs (3 mM) AzoTP, AzoethoxyTP, DimethylazoTP and AzoethylTP induced fibre shortening. Black, red, green, blue and pink circles represent the % length change induced by ATP, AzoTP, AzoethoxyTP, DimethylazoTP and AzoethylTP respectively; the lines are best-fit through the data trend. Error bars: standard deviation for 4 fibres.

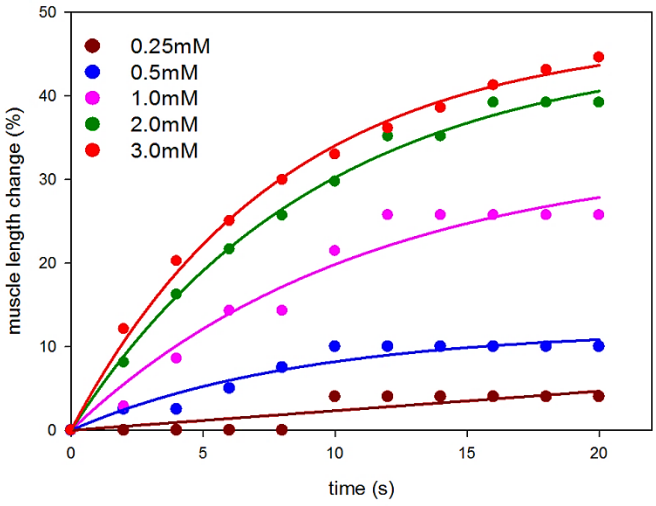

Figure 10. Shortening of glycerinated muscle fiber with respect to the concentration of AzoTP. Lines are best fit through the data trend.

4. CONCLUSION

In a step towards employing our AzoTP energy molecules to regulate the macroscopic systems, we have demonstrated the photo-regulated initiation of shortening in glycerinated skeletal muscle fibre induced by the photoisomerization. Direct irradiation with visible light initiated the shortening in the inactive *cis*-AzoTPs infused muscle fibre by locally photo-generated *trans*-AzoTPs. The *trans* form of AzoTPs initiates the contraction and shortens the muscle fibre to almost half of its initial length, whilst *cis* isomer's contribution is insignificant. Also, we demonstrated the functionality of AzoTP as an efficient substrate for myosin motor in addition to kinesin as reported previously, thus implying its generalizability for cytoskeletal motors. The newly designed and synthesized three AzoTPs serve as the substrate for myosin motor and photoregulate the motility at molecular as well as macroscopic level. All the four AzoTP molecules drive myosin triggered *in-vitro* gliding velocity of F-actin with 50 to 60% efficiency of that obtained with ATP and photo-control the velocity between fast/slow states by undergoing photoisomerization. The demonstration of the photocontrol of macroscopic glycerinated muscle fibre system is a promising indication towards regulating the much complex intact *in vivo* systems and organisms by utilizing photoresponsive energy molecules. The regulation of complex biological systems could benefit in investigating the disorders and targeted drug delivery. Efficient functionality of our AzoTP molecules in myosin-actin and kinesin-microtubule motile system at molecular as well as macroscopic level makes them interesting photoswitches which could find potential in various biomolecular tasks.

5. REFERENCES

1 R. D. Vale, *Cell*, 2003, 112, 467–480.

2 R. D. Vale, *Science*, 2000, 288, 88–95.

3 G. D. Bachand, N. F. Bouxsein and V. Vandelinder, *WIREs Nanomed Nanobiotechnol* 2014, 6, 163–177.

4 N. V Delrosso and N. D. Derr, *Curr. Opin. Biotechnol.*, 2017, 46, 20–26.

5 M. Schliwa and G. Woehlke, *Nature*, 2003, 422, 759–765.

6 A. Goel and V. Vogel, *Nat. Nanotechnol.*, 2008, 3, 465–475.

7 T. Korten, A. Mansson and S. Diez, *Curr. Opin. Biotechnol.*, 2010, 21, 477–488.

8 L. Chen, M. Nakamura, T. D. Schindler, D. Parker and Z. Bryant, *Nat. Nanotechnol.*, 2012, 7, 252–256.

9 H. Higuchi, E. Muto, Y. Inoue and T. Yanagida, *Proc. Natl. Acad. Sci. U. S. A.*, 1997, 94, 4395–4400

10 H. Hess, J. Clemmens, D. Qin, J. Howard, V. Vogel, *Nano Lett.*, 2001, 1, 235–239.

11 D. Wu, R. Tucker and H. Hess, *IEEE Trans. Adv. Packag.*, 2005, 28, 594–599.

12 T. Kamei, T. Fukaminato and N. Tamaoki, *Chem. Commun.*, 2012, 48, 7625-7627.

13 N. Perur, M. Yahara, T. Kamei and N. Tamaoki, *Chem. Commun. (Camb).*, 2013, 49, 9935–9937.

14 P. Y. Bolinger, D. Stamou and H. Vogel, *Angew. Chemie - Int. Ed.*, 2008, 47, 5544–5549.

15 C. V. Rao and A. P. Arkin, *Annu. Rev. Biomed. Eng.*, 2001, 3, 391–419.

16 E. Thedinga, N. Karim, T. Kraft and B. Brenner, *J. Muscle Res. Cell Motil.*, 1999, 20, 785–796.

17 F. Von Wegner, S. Schurmann, R. H. A. Fink, M. Vogel and O. Friedrich, *IEEE Trans. Med. Imaging*, 2009, 28, 1632–1642.

18 S. J. Kron and J. a Spudich, *Proc. Natl. Acad. Sci. U. S. A.*, 1986, 83, 6272–6276.

19 Y. Y. Toyoshima, S. J. Kron, E. M. McNally, K. R. Niebling, C. Toyoshima and J. A. Spudich, *Nature*, 1987, 328, 536–539.

20 R. Cooke and W. Bialek, *Biophys. J.*, 1979, 28, 241–258.

21 H. E. Huxley, *Nature*, 1973, 243, 445–449.

22 R. Cooke and K. C. Holmes, *Crit Rev Biochem Mol Biol*, 1986, 21, 53-118.

23 A. G. Szent-Györgyi, *J. Gen. Physiol.*, 2004, 123, 631–641.

24 A. M. Gordon, E. Homsher and M. Regnier, *Physiol. Rev.*, 2000, 80, 853–924.

25 R. Stehle, J. Solzin, B. Iorga and C. Poggesi, *Pflugers Arch. Eur. J. Physiol.*, 2009, 458, 337–357.

26 C. Hoppmann, P. Schmieder, P. Domaing, G. Vogelreiter, J. Eichhorst, B. Wiesner, I. Morano, K. Rück-Braun and M. Beyermann, *Angew. Chemie - Int. Ed.*, 2011, 50, 7699–7702.

27 I. Rayment, W. R. Rypniewski, K. Schmidt-Base, R. Smith, D. R. Tomchick, M. M. Benning, D. A. Winkelmann, G. Wesenberg and H. M. Holden, *Science*, 1993, 261, 50–58.

28 I. Rayment, H. Holden, M. Whittaker, C. Yohn, M. Lorenz, K. Holmes and R. Milligan, *Science*, 1993, 261, 58–65.

29 A. J. Fisher, C. A. Smith, J. B. Thoden, R. Smith, K. Sutoh, H. M. Holden and I. Rayment, *Biochemistry*, 1995, 34, 8960–8972.

30 H. D. White, B. Belknap and W. Jiang, *J. Biol. Chem.*, 1993, 268, 10039–10045.

31 E. Pate, K. Franks-Skiba, H. White and R. Cooke, *J. Biol. Chem.*, 1993, 268, 10046–10053.

32 J. C. Grammer, H. Kuwayama and R. Yount G, *Biochemistry*, 1993, 32, 5725–5732.

33 Kay L. Nakamaye, James A. Wells, Robert L. Bridenbaugh, Yoh Okamoto and Ralph G. Yount, *Biochemistry*, 1985, 24, 5226-5235.

34 S. S. Margossian and S. Lowey, *Methods Enzymol.*, 1982, 85, 55–71.

35 J. D. Pardee and J. Aspudich, *Methods Enzymol.*, 1982, 85, 164–181.

36 S. J. Kron, Y. Y. Toyoshima, T. Q. P. Uyeda and J. A. Spudich, *Methods Enzymol.*, 1991, 196, 399–416.

37 E. Meijering, O. Dzyubachyk and I. Smal, *Methods Enzymol.*, 2012, 504, 183–200.

38 A. Szent-Gyorgyi, *Biol. Bull.*, 1949, 96, 140–161.

LIST OF PUBLICATIONS

1). Halley M. Menezes, Md. Jahirul Islam, Masayuki Takahashi and Nobuyuki Tamaoki. 'Driving and photo-regulation of myosin–actin motors at molecular and macroscopic levels by photo-responsive high energy molecules'. ***Org. Biomol. Chem.***, 2017, **15**, 8894-8903

ACKNOWLEDGMENTS

I thank the Lord almighty for the choicest blessings and grace.

My supervisor, Professor Nobuyuki Tamaoki has been a constant source of support, prompt guidance, scientific ideas and valuable suggestions throughout my doctoral study. My heartfelt thanks to him, for this work would not have been possible without his support, guidance and immense knowledge. I am forever grateful to him for the unflinching encouragement, patience and fruitful research memories.

I am humbly grateful to Professor Masayuki Takahashi for all the encouragement, support and training me in protein preparations.

My sincere gratitude to Assistant Professors, Dr. Kazuya Matsuo, Dr. Yoshimitsu Sagara, Dr. Yuna Kim, Dr. Takashi Kamei and Dr. Tsuyoshi Fukaminato for their warm encouragement and involvement through important suggestion and discussions.

I thank all my former and present fellow labmates, for the stimulating discussions, for the times we were working together and for all the fun we have had during my course. I specially acknowledge the motivation and cooperation of Md. Jahirul Islam in completing this thesis.

I am thankful to our group secretaries Hiroko Tayama, Mariko Ooki and Arisa Hirade for their indispensable help in dealing with scholarship and administration processes during my course.

I am indebted to Hokkaido University and IGP-RPLS for providing me the opportunity to study in Japan and explore this amazing country. I am grateful to

MEXT and JASSO for providing scholarships that made my study and stay here smoother.

I have been lucky to be blessed with many friends during my stay here, my heartfelt thanks to all for the love, affection and unforgettable memories. My special thanks to Deepak H.V and Desi Utami for the unending support.

I thank Professor C. B. Yellamagad for instilling the interest towards research and motivating me to pursue the PhD.

My family deserves special mention for their everlasting love, support and good wishes. I am eternally grateful to my parents for being the pillar of my strength and my brothers for all the support. I also thank my friends back in India, Dr. Vidyasagar, Dr. Gayatri and Dr. Laveena for their constant support.